PIONEER Data Acquisition Development

Jack Carlton
University of Kentucky

Outline

I. [3-17] What is PIONEER?
   A. Physics Background
   B. Experimental Design
II. [18-23] Test stand DAQ Development
   A. Hardware Description
   B. Software Adjustments
III. [24-30] 2023 PSI Test Beam
   A. Experiment Description
   B. Results
IV. [31-41] PIONEER DAQ Development
   A. Proposed Framework
   B. Prototyping
   C. Compression
V. [42-46] Current and Future Work

What is PIONEER?

j.carlton@uky.edu

$\pi \rightarrow e\nu_e$ and $\pi \rightarrow \mu\nu_\mu$

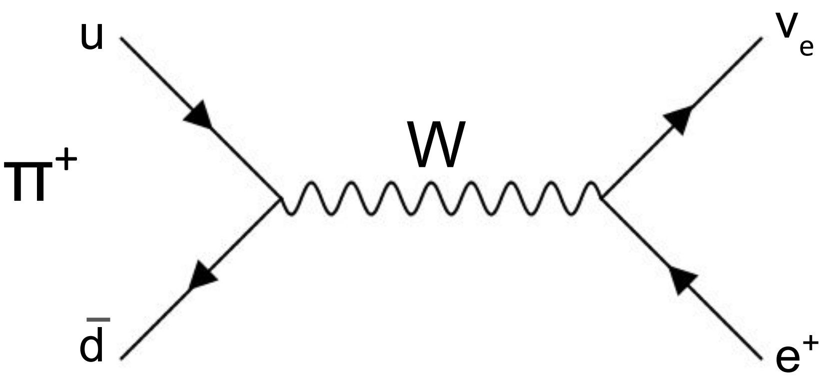

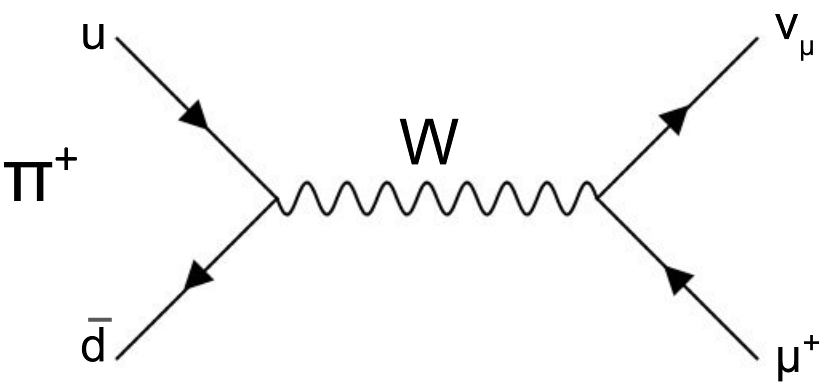

- Corresponding diagrams for π^-
- Tau decay forbidden
  - tau too massive ~ 1000 MeV/c^2
  - Pion ~ 100 MeV/c^2
- Muon decay more likely
  - branching fraction of 0.999877

Helicity Suppression (Why is Muon Decay Most Likely?)

- Naively, $\Gamma \propto p'$ → electron decay more likely
- Weak force only affects left-handed (LH) chiral particle states and right-handed (RH) chiral anti-particle states
- Neutrinos are all LH chirality
- m_ν << E means LH neutrino chirality→ LH (negative) neutrino helicity
- Conservation of momentum → anti-lepton is LH (negative) helicity

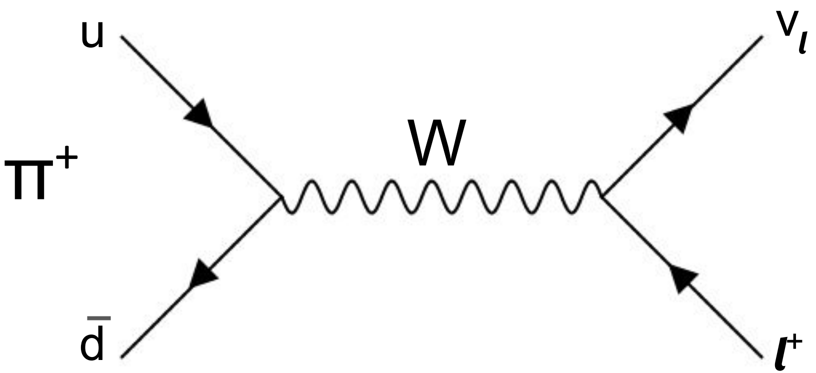

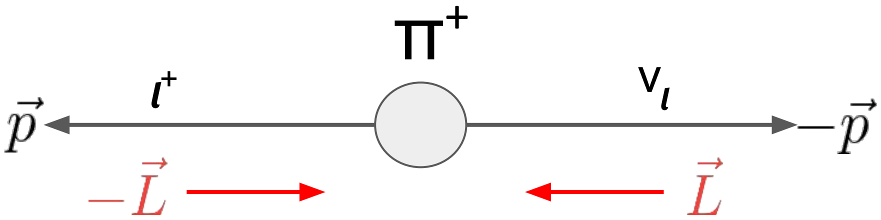

j.carlton@uky.edu

Helicity Suppression (Why is Muon Decay Most Likely?)

- We can write the LH (negative) helicity anti-particle state in the chiral basis:

$$v_{\downarrow} = \frac{A}{2}\left[\left(1 - \frac{p}{E+m}\right) v_R - \left(1 + \frac{p}{E+m}\right) v_L\right]$$

- We ignore the LH term (weak force only acts on the RH term), anti-particle's matrix element contribution:

$$\mathcal{M} \sim \frac{1}{2}\left(1 - \frac{p_l}{E_l + m_l}\right) \xrightarrow[m_\nu \to 0]{} \frac{m_l}{m_\pi + m_l}$$

- This effect ends up making the matrix element smaller → decay rate smaller

$$\Gamma \propto |\mathcal{M}|^2$$

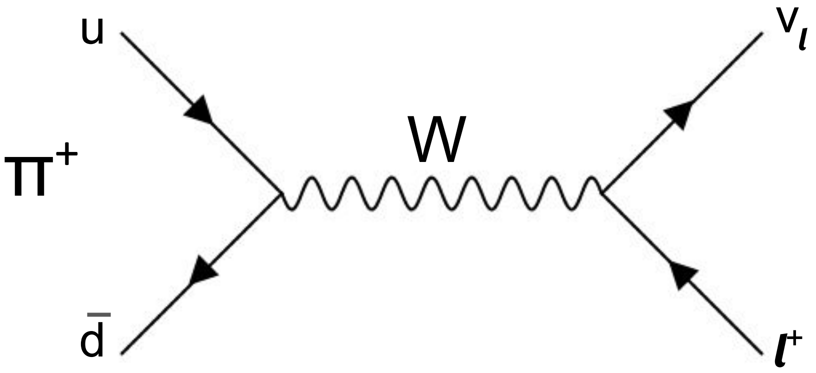

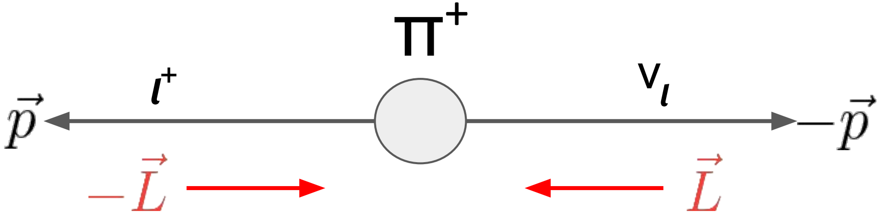

j.carlton@uky.edu

Lepton Universality

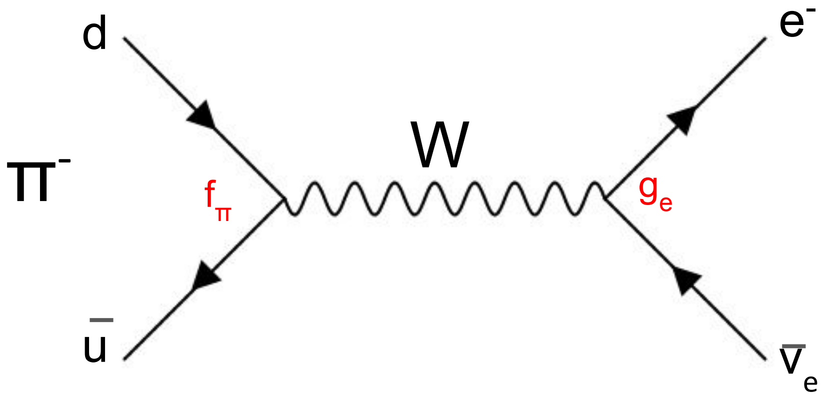

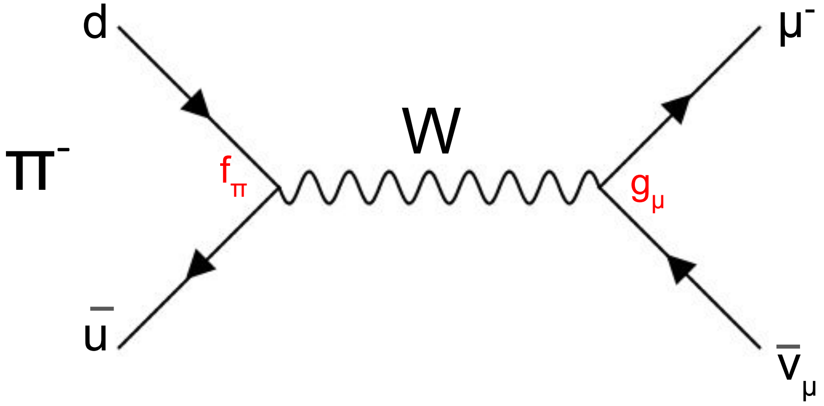

- States coupling strengths (vertices) $g_e = g_\mu = g_\tau$
- Using the Feynman rules for the weak interaction, we can approximate the matrix element

$$\mathcal{M}_{fi} = \underbrace{\left[\frac{g_W}{\sqrt{2}}\frac{1}{2}f_\pi p_\pi^\alpha\right]}_{\text{Pion vertex}} \cdot \underbrace{\left[\frac{g_{\alpha\beta}}{m_W^2}\right]}_{\text{W-boson propagator}} \cdot \underbrace{\left[\frac{g_W}{\sqrt{2}} g_l \bar{u}(p_l)\gamma^\beta \frac{1}{2}(1-\gamma^5)v(p_\nu)\right]}_{\text{Lepton vertex}}$$

j.carlton@uky.edu

Lepton Universality

- After some "massaging" we can find the matrix element to be

$$\mathcal{M}_{fi} = \left(\frac{g_W}{2m_W}\right)^2 f_\pi g_l \cdot \sqrt{m_\pi^2 - m_l^2}$$

- Pion spin zero → no spin averaging needed, i.e.:

$$\langle|\mathcal{M}_{fi}|^2\rangle = |\mathcal{M}_{fi}|^2 = \left(\frac{g_W}{2m_W}\right)^4 f_\pi^2 g_l^2 \cdot (m_\pi^2 - m_l^2)$$

- We can use the general formula for 2-body decay to to find the decay rate

$$\Gamma = \frac{p\langle|\mathcal{M}_{fi}|^2\rangle}{8\pi m_\pi^2} = \frac{f_\pi^2}{16\pi^2 m_\pi^3}\left(\frac{g_W}{2m_W}\right)^4 \left[m_l g_l (m_\pi^2 - m_l^2)\right]^2$$

- Finally, we compute the branching ratio

$$\frac{\Gamma(\pi^- \to e^-\bar{\nu}_e)}{\Gamma(\pi^- \to \mu^-\bar{\nu}_\mu)} = \left(\frac{g_e}{g_\mu}\right)^2 \left[\frac{m_e(m_\pi^2 - m_e^2)}{m_\mu(m_\pi^2 - m_\mu^2)}\right]^2$$

Lepton Universality

$$\frac{\Gamma(\pi^- \to e^- \bar{\nu}_e)}{\Gamma(\pi^- \to \mu^- \bar{\nu}_\mu)} = \left(\frac{g_e}{g_\mu}\right)^2 \left[\frac{m_e(m_\pi^2 - m_e^2)}{m_\mu(m_\pi^2 - m_\mu^2)}\right]^2$$

- Lepton universality assumes $g_e = g_\mu$, so the first factor disappears
- Improving the branching ratio measurement and comparing to the theoretical value acts as a test of lepton universality
- Another test would consider pure leptonic decays, but such decays involving taus are too rare for high precision measurements

j.carlton@uky.edu

Branching Ratio $R_{e/\mu}$

- We can measure the branching ratio by measuring # of decays e and μ decays

$$R_{e/\mu} \equiv \frac{\Gamma(\pi^- \to e^- \bar{\nu}_e)}{\Gamma(\pi^- \to \mu^- \bar{\nu}_\mu)}$$

- Theoretical prediction is simple in first (and second) order
  - No f_π or CKM element V_{ud}

$$R^0_{e/\mu} = \left(\frac{g_e}{g_\mu}\right)^2 \left[\frac{m_e(m_\pi^2 - m_e^2)}{m_\mu(m_\pi^2 - m_\mu^2)}\right]^2$$

= 1 [in theory]

- 3rd order correction and beyond the pion structure becomes relevant

$$R^{(\text{theory})}_{e/\mu} = R^0_{e/\mu}\left(1 - \frac{3\alpha}{\pi}\ln\left(\frac{m_\mu}{m_e}\right) + \ldots\right)$$

Current state of $R_{e/\mu}$

$$R_{e/\mu}^{exp} = 1.2327(23) \times 10^{-4} \text{ (PIENU collab)}$$

$$R^{theo} = 1.23524(15) \times 10^{-4}$$

- Consistent with each other
- Expect factor of ~10 precision improvement on experimental value from PIONEER
  - “Catches up” with theoretical uncertainty

Past Experimental Approach (PIENU)

- NaI has a long primary decay time
  - ~ 250 ns
- Event pileup forces the experiment to run at a low rate
  - ~70 kHz
- “inactive target”, muons aren’t tracked
- CsI Rings for shower leakage detection

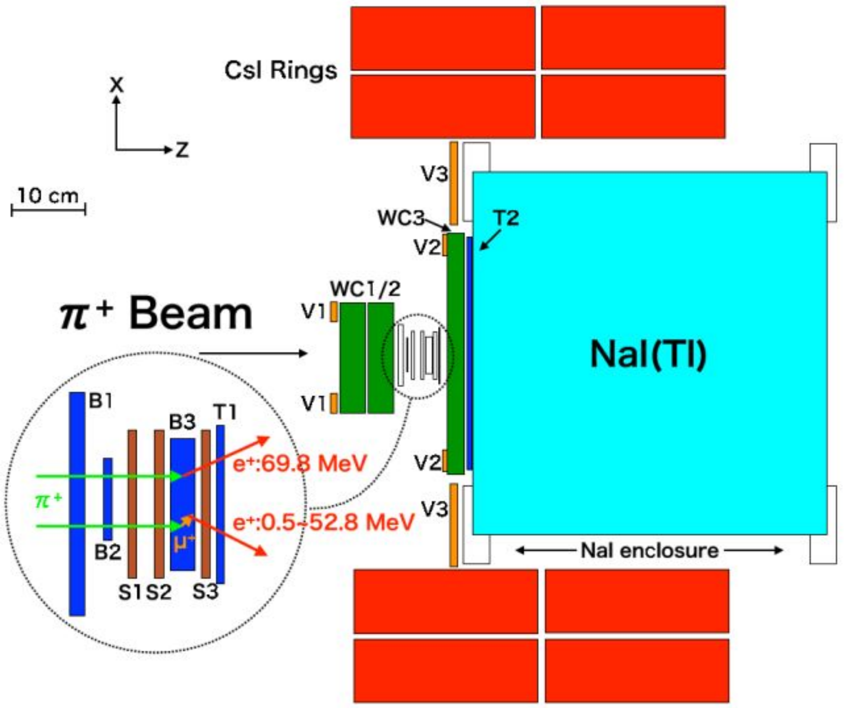

PIONEER Experimental Proposal

- LXe (or LYSO) has shorter decay time
  - ~ 25 ns
- Allows experiment to run at much higher rate
  - ~300kHz (phase 1)
  - ~2000kHz (phase 2 and 3)
- “active target”, muons and pions are “tracked”

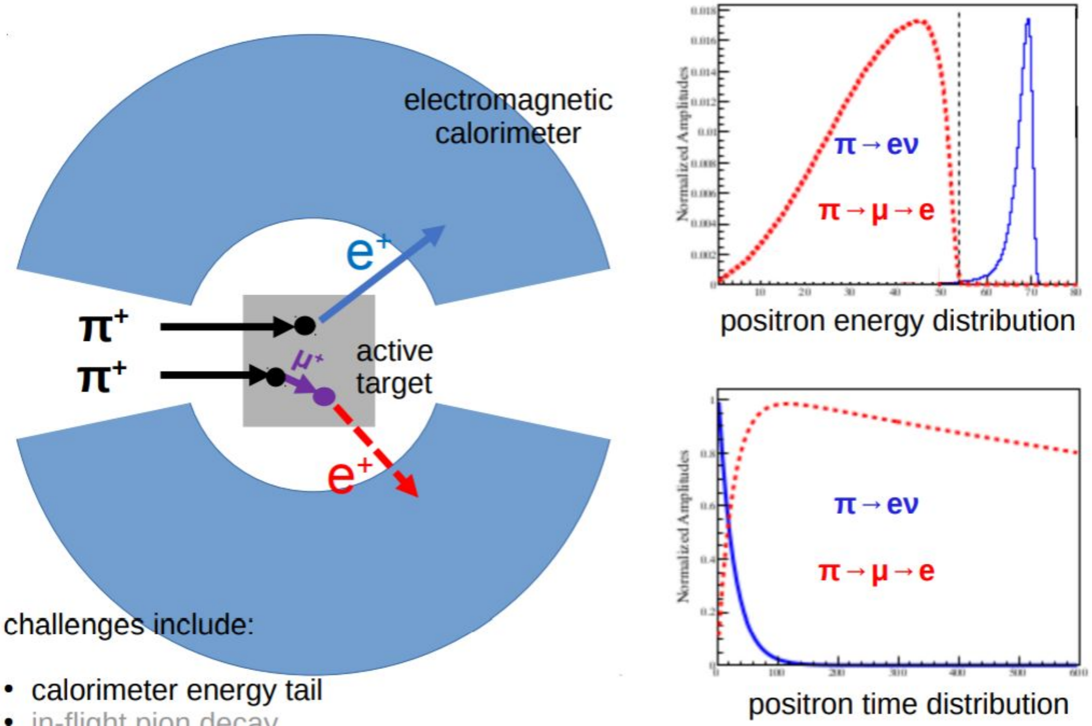

challenges include:

- calorimeter energy tail
- in-flight pion decay
- beam, positron pileup

3D Render Experiment

Not Pictured:

- ATAR (inside Calo)
- Tracker (a shell around ATAR, inside Calo)
- VETOs, T0, etc.
- DAQ Computers

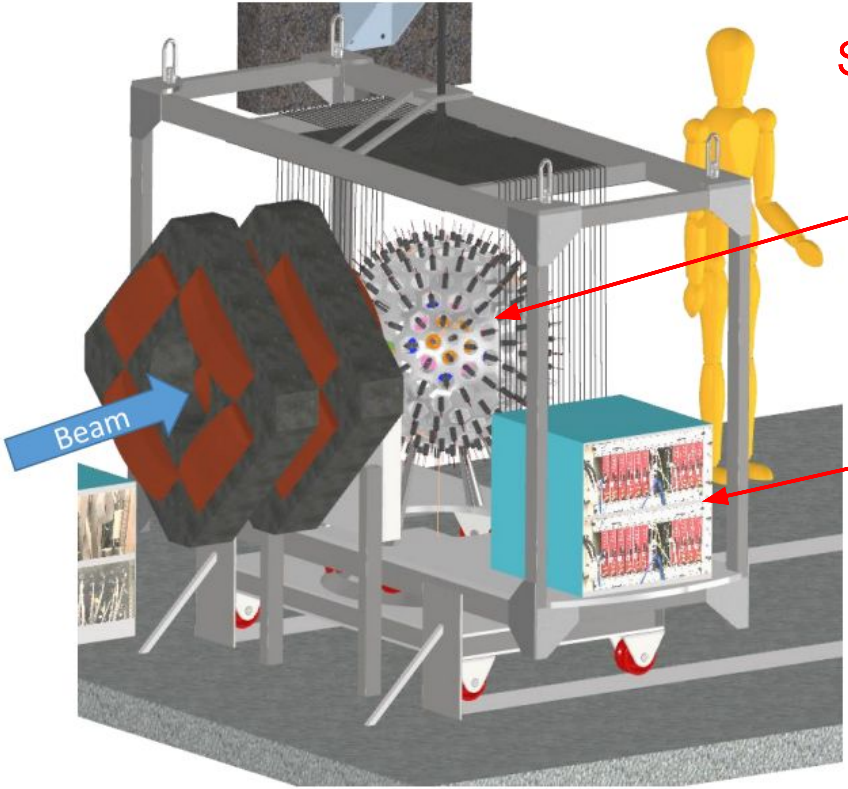

Spherical Calorimeter Design

Digitization Electronics

j.carlton@uky.edu

Calorimeter (CALO) Purpose

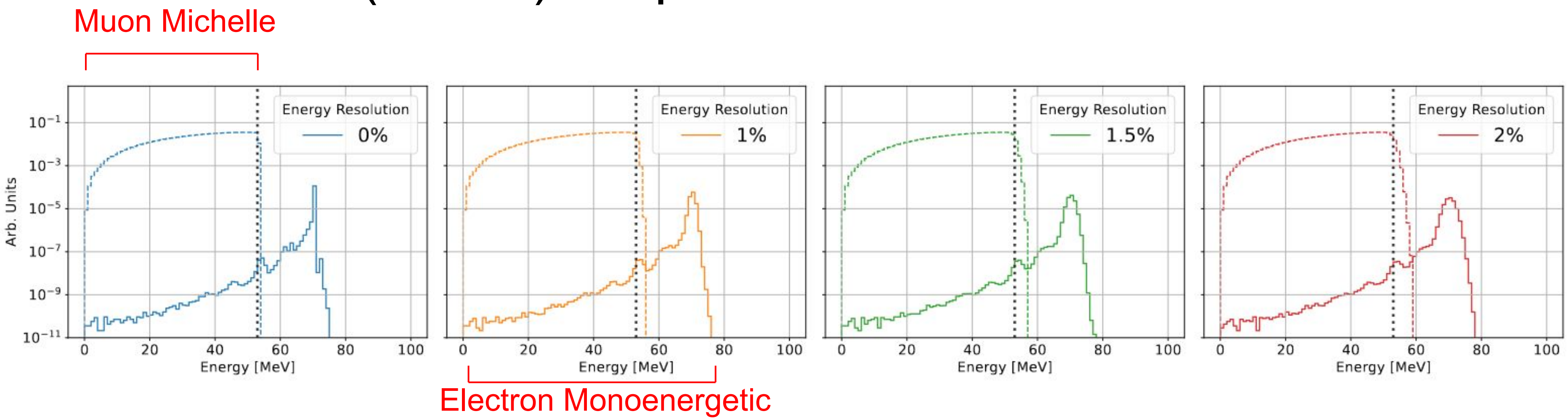

- Muon’s intrinsically follow a Michelle Spectrum
  - Additionally width comes from energy resolution
- Positrons follow monoenergetic spectrum
  - “Back” and “Front” tail due to radiative decays and bremsstrahlung
- Good energy resolution is crucial for event reconstruction

Active Target (ATAR) Purpose

arxiv: 2203.01981

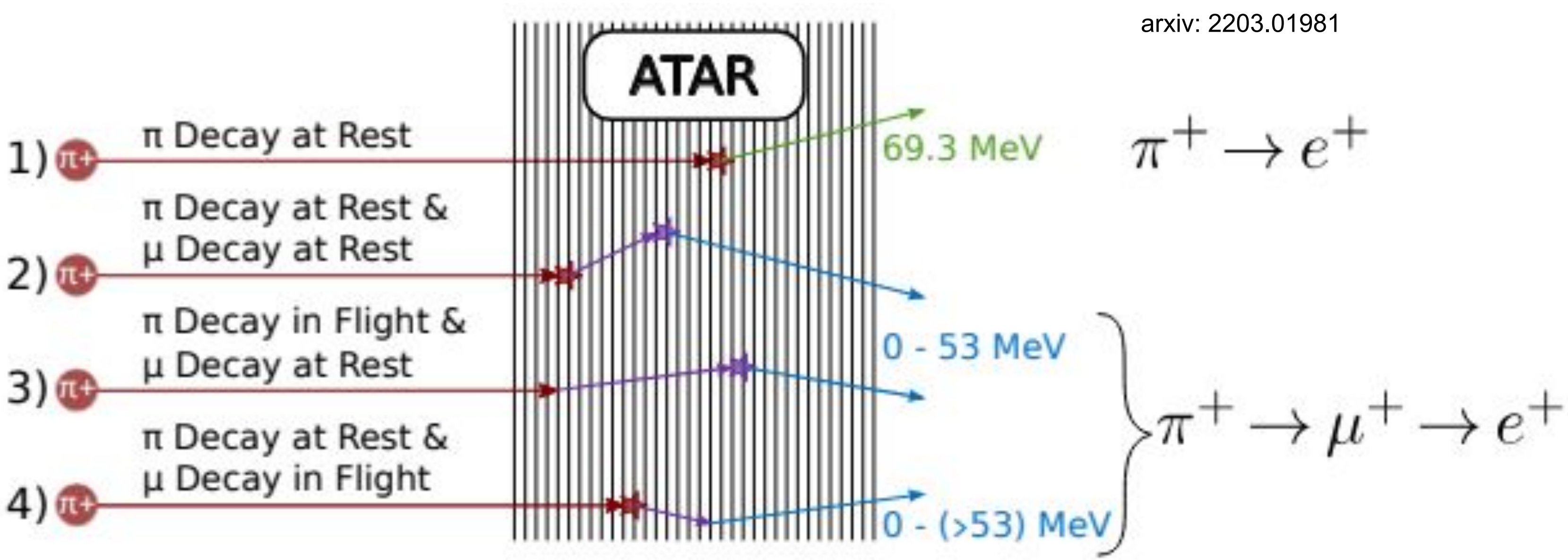

Midas Framework

- C/C++ (mostly) package of modules for
  - run control,
  - expt. configuration
  - data readout
  - event building
  - data storage
  - slow control
  - alarm systems
  - Etc.
- Can link with custom software

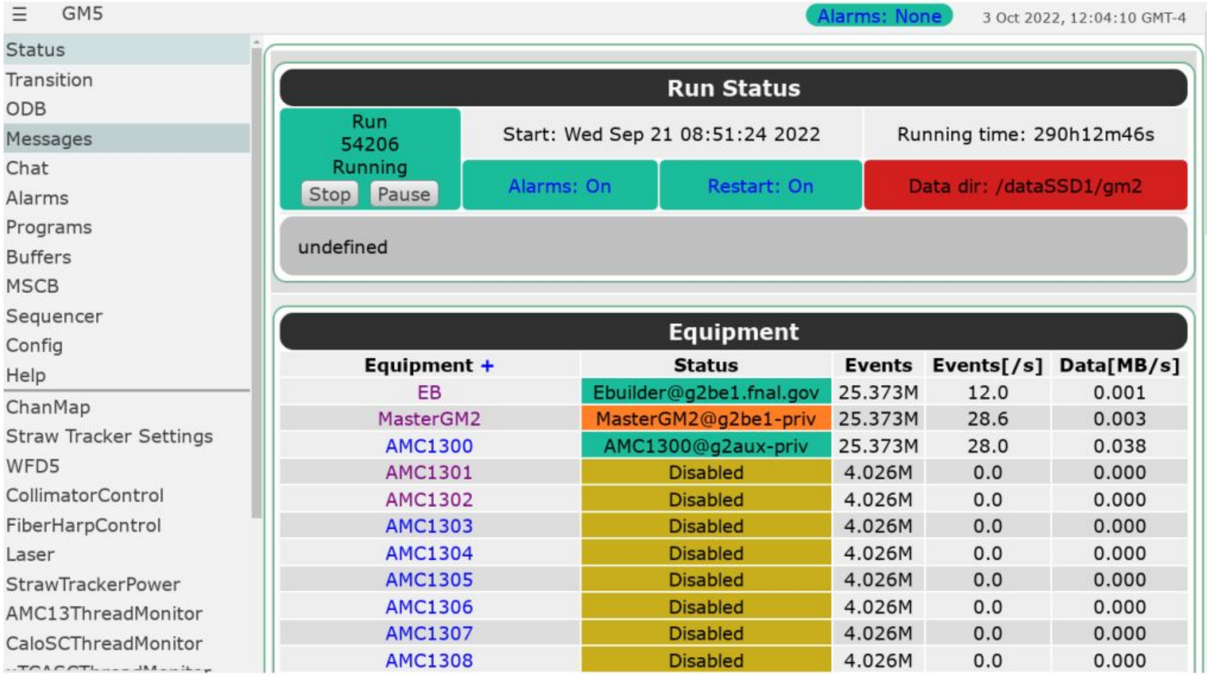

Example g-2 Midas Webpage

Test stand DAQ Development

Overview

- The test stand DAQ is used throughout the PIONEER collaboration
    - Helps test and develop crucial experiment components
- Built on top of g-2 DAQ hardware and software

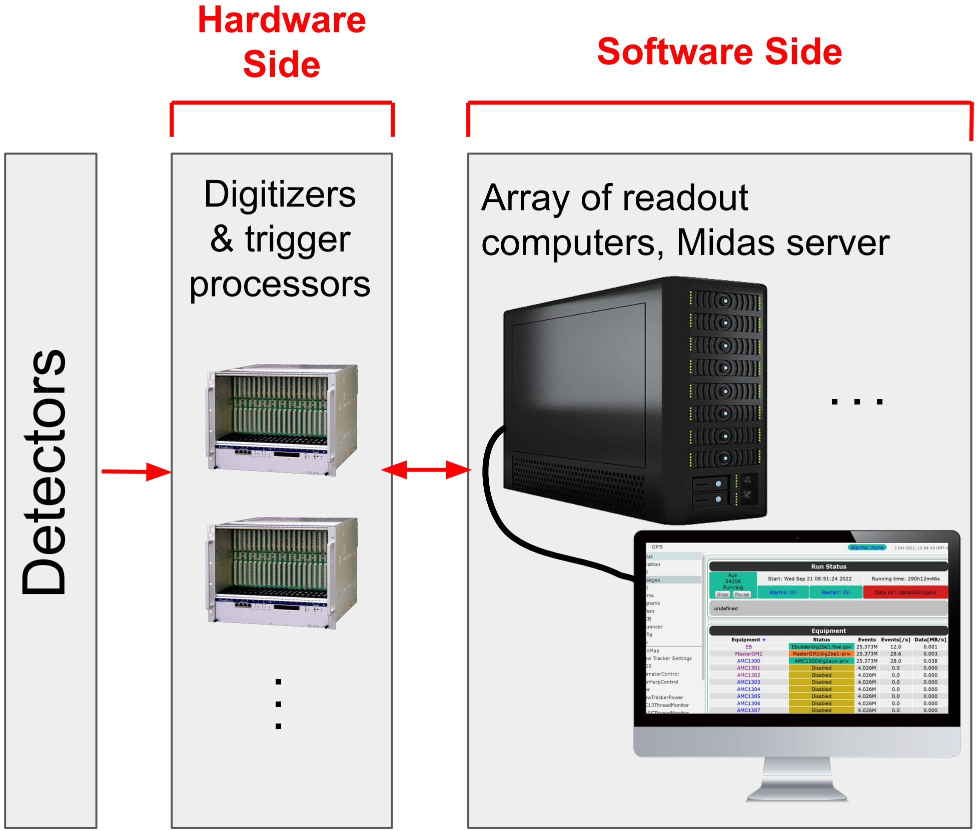

Hardware - Labeled Crate

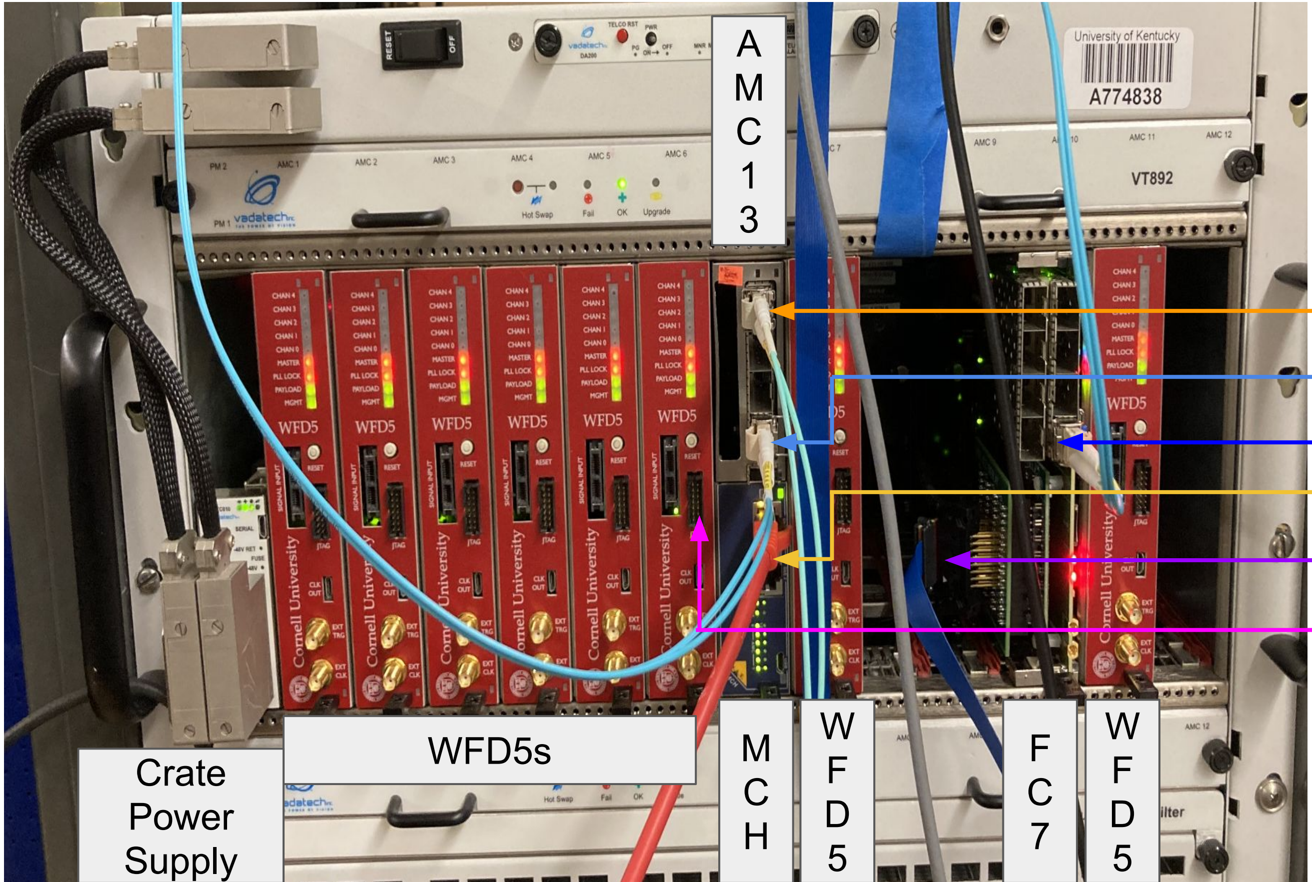

<u>Note:</u> AMC13 and MCH are half slot modules

10GbE out (data) AMC13→desktop

Trigger in AMC13

Trigger out FC7

1GbE MCH in/out (comm.)

FC7 Trigger in

WFD5 5-channel, differential signal in (no connection in this picture)

Software - Adjustment Made

- Generalized the frontend code
  - Crate contents no longer assumed
  - Added option to remove unneeded hardware reliance (meinberg card)
  - Added support for arbitrary number of crates
  - Added scripts for ease of setup and use

- Added features
  - Timing monitoring
  - Data quality Monitoring (DQM)
  - System resource monitoring

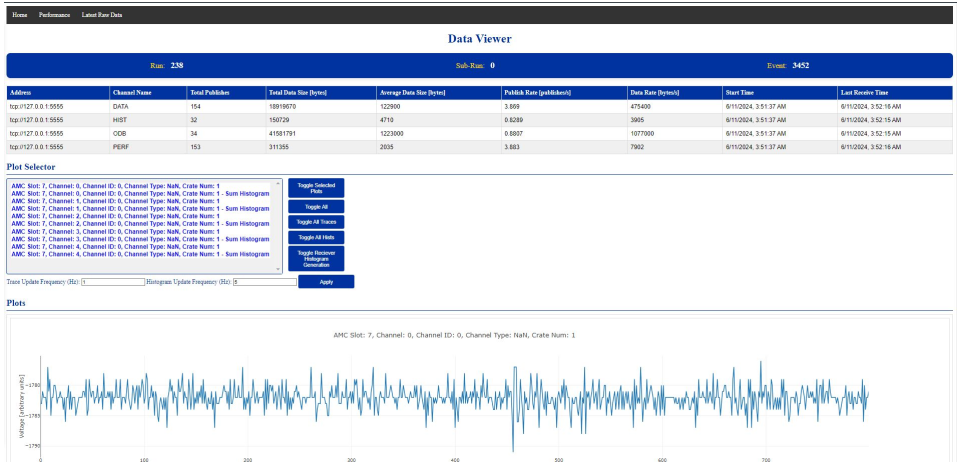

Generalized Teststand DAQ DQM Webpage

j.carlton@uky.edu

Documentation

- Setup of the teststand DAQ is not straightforward
  - Custom software and hardware
  - Specific software and hardware configurations
- Created documentation to aid users
  - Website version on github pages https://jaca230.github.io/teststand_daq_manual/

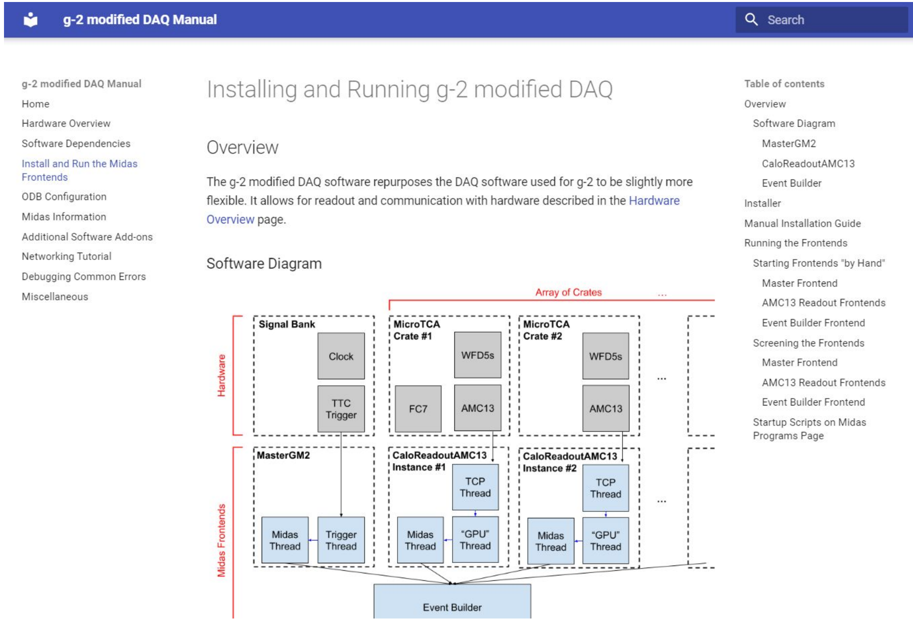

A page from the manual webpage

Use Cases

- LYSO tests at CENPA
- 2023 PSI Test Beam
- Liquid Xenon tests at TRIUMF
- Experiments at PSI

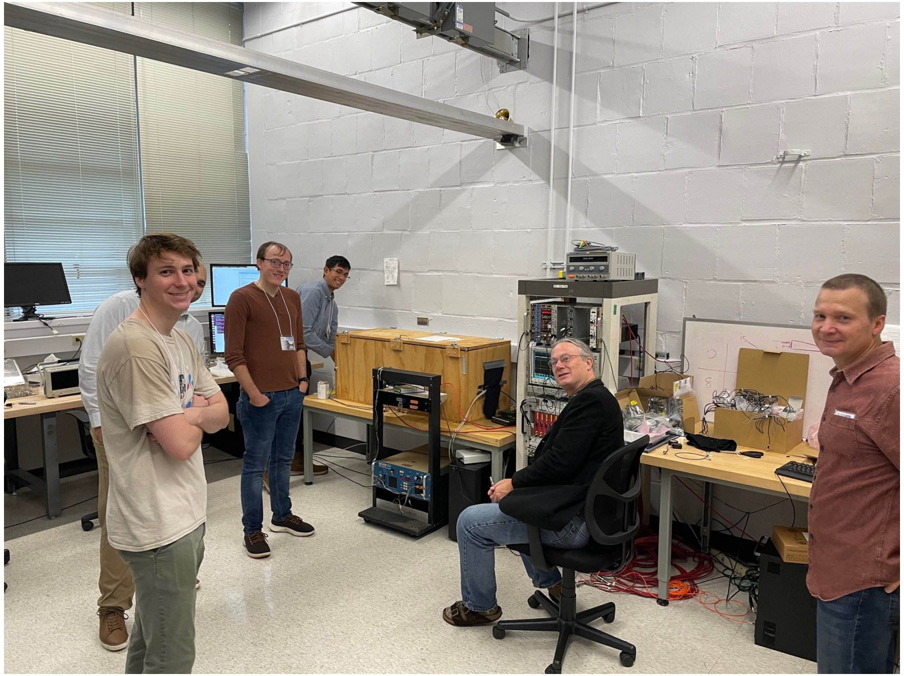

Setting up test stand at University of a Washington (on a rainy day)

2023 PSI Test Beam

Overview

- PIONEER LYSO Calorimeter test
  - November 15 - 29, 2023

- Made measurements using LYSO scintillator crystals to determine if they are an adequate candidate for PIONEER’s calorimeter
  - **Energy resolution**
  - Timing resolution
  - Spatial resolution

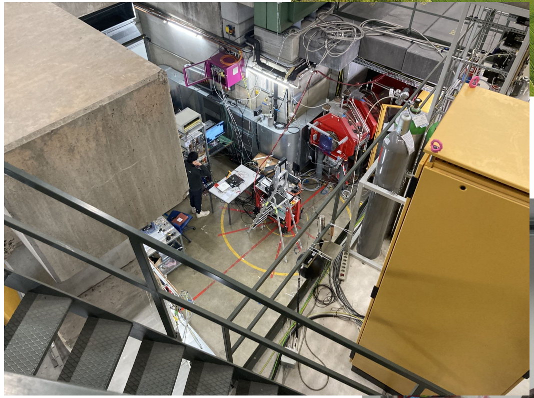

Experiment Diagram - Conceptual Picture

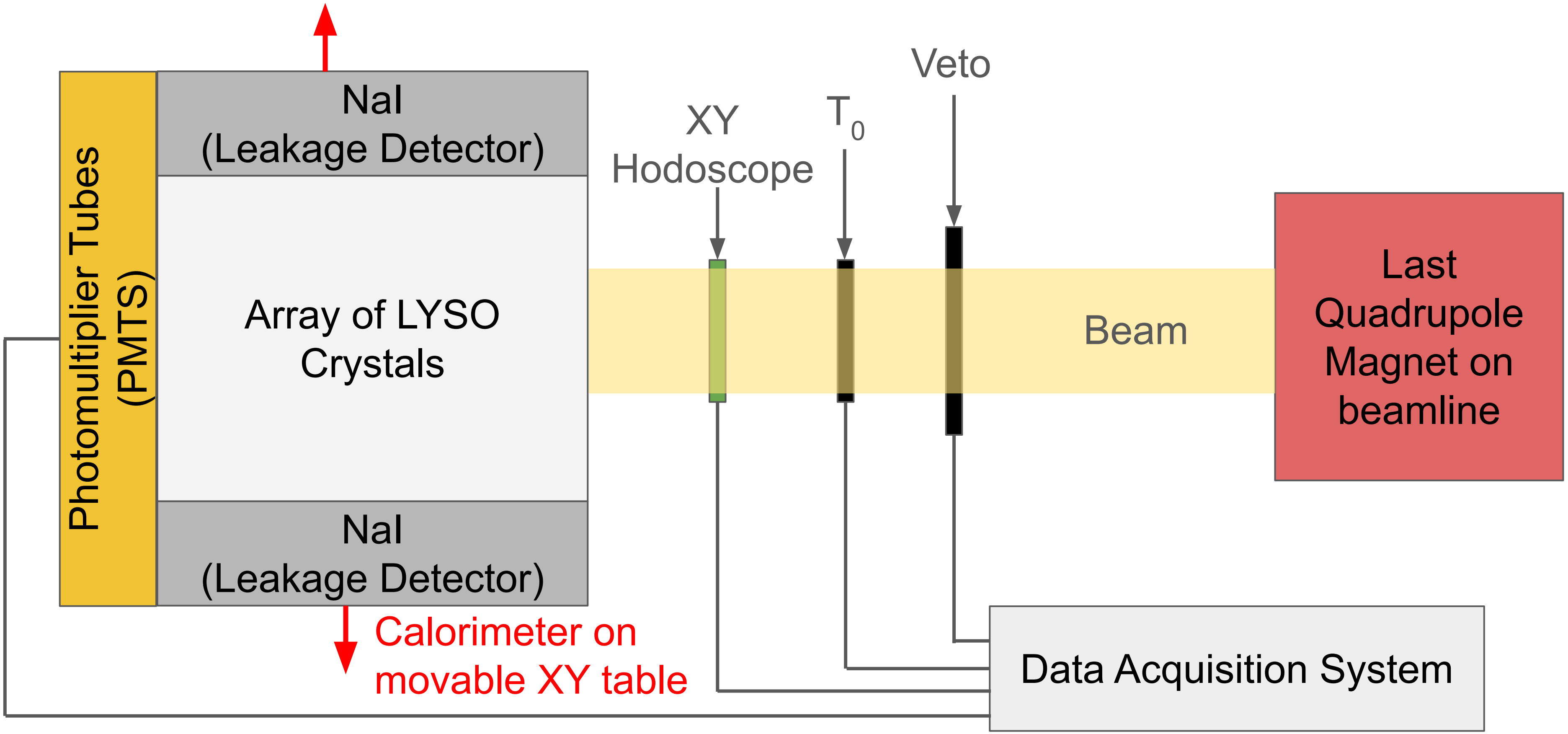

Experiment Diagram - Labeled Picture

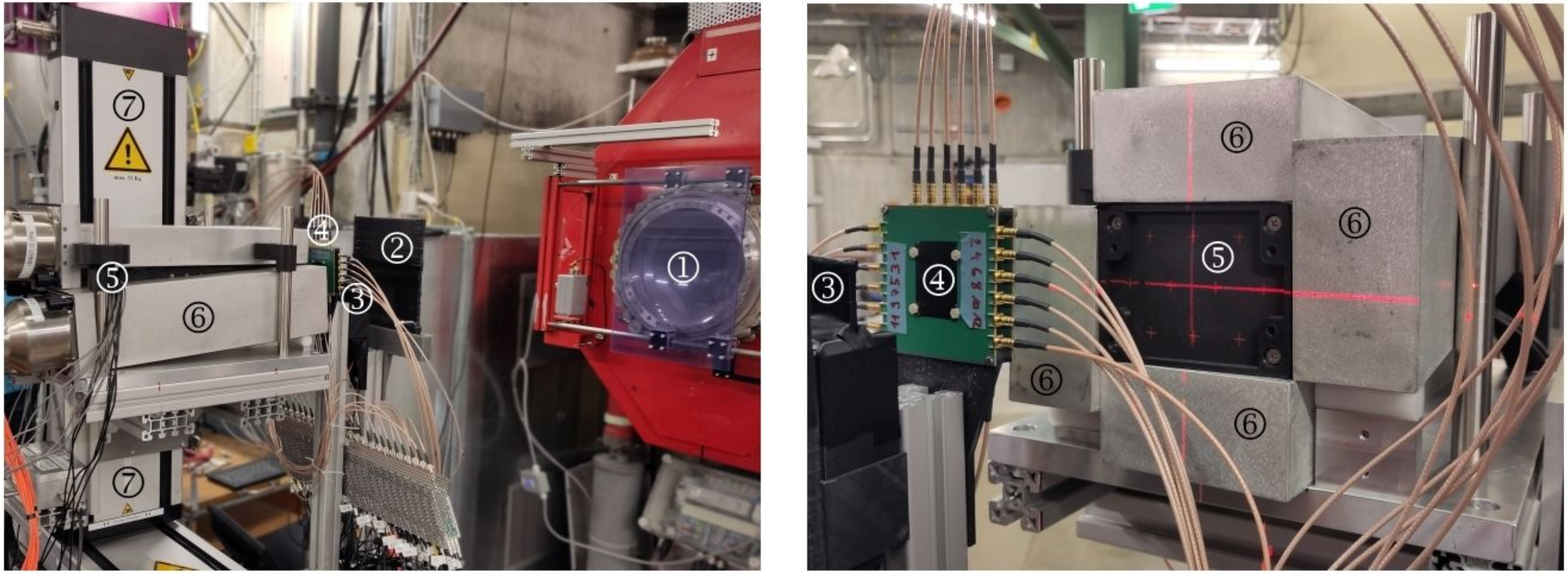

(a) (b)

A full view of the detector setup during the PSI test beam (a) and a close-up of the calorimeter front-face during laser alignment (b). Positrons from the last quadrupole magnet ① pass through the VETO counter ②, T0 ③, and beam hodoscope ④ before depositing energy in the LYSO array ⑤. The LYSO crystals, along with the surrounding NaI detectors ⑥, are mounted on a movable XY table ⑦.

LYSO Calorimeter

- Constructed from an array of 10 LYSO crystals
  - NaI for leakage detection
- $X_0 = 1.14$ cm
- $R_M = 2.07$ cm

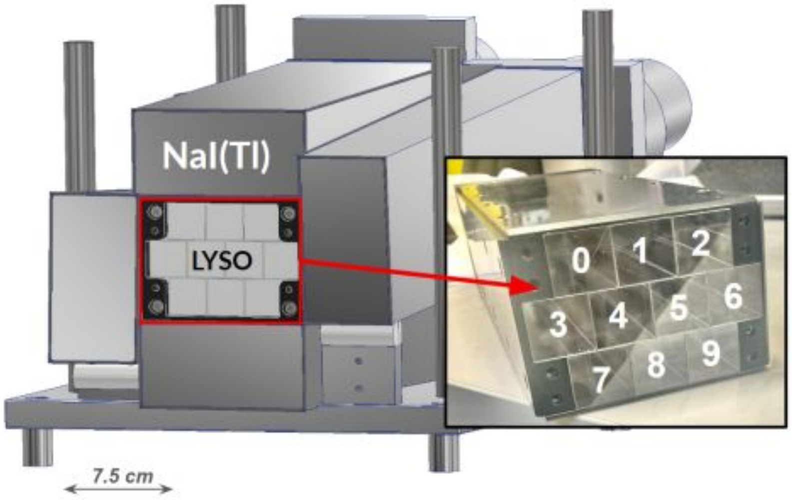

Front-facing image of LYSO calorimeter

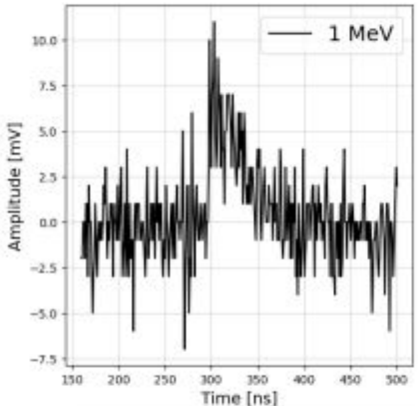

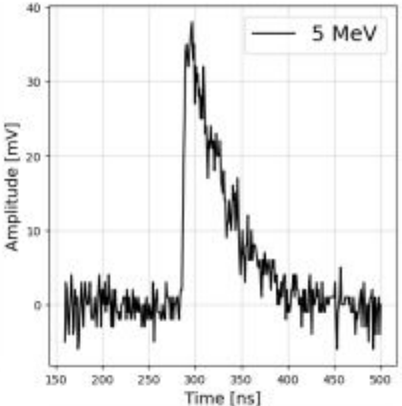

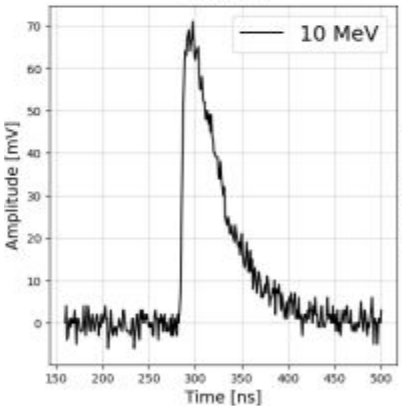

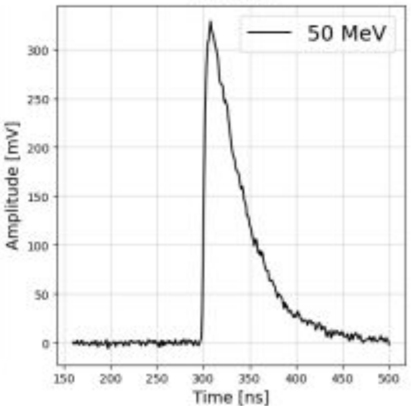

Hodoscope

- 2 Layers of 12 scintillator strips
  - Layers offset by 90 degrees
- 2 mm x 2 mm "pixels" created by strip intersections
  - Allows for finer positioning data

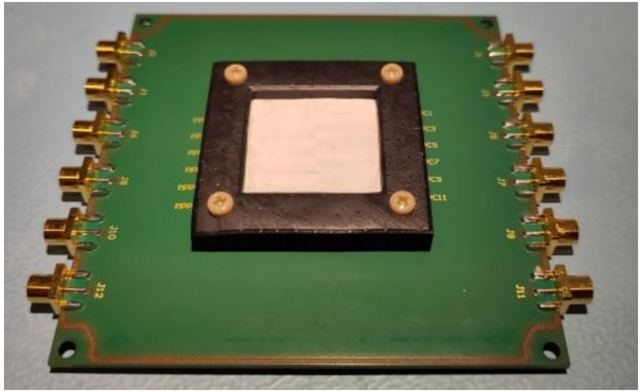

1 Hodoscope layer, 12 SiPMs connecting to 12 BC404 plastic scintillator 2mm wide bars

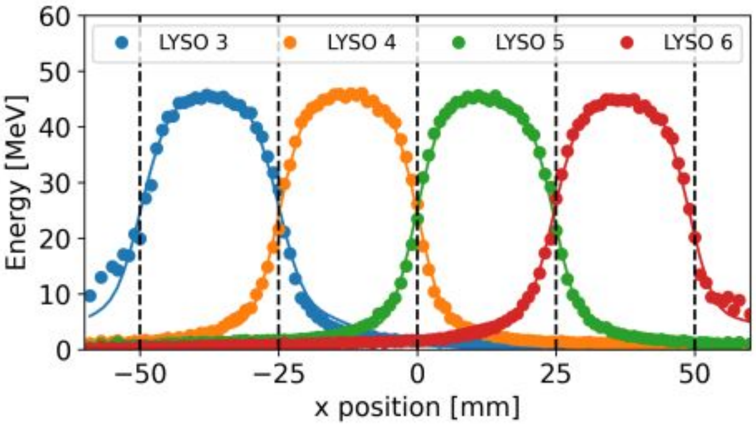

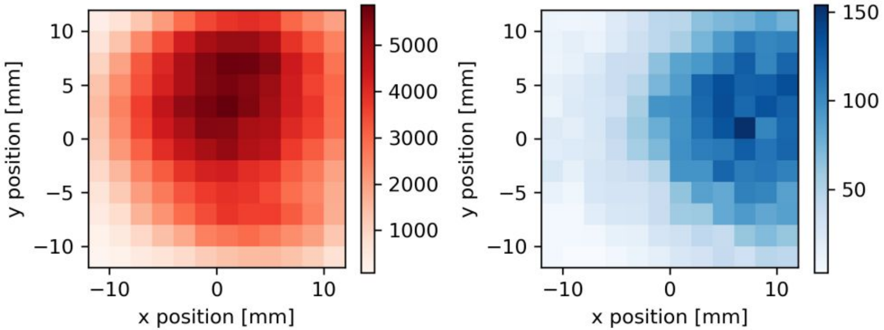

Beam Profile: Red - positrons, Blue - muons

Results - Energy Resolution

- Measured an energy resolution of **ΔE/E = 1.55 ± 0.05%**
  - Published as 1.80, recently improved with better integration strategy
  - 70 MeV ≈ e energy in $\pi \rightarrow e\nu_e$

- Over two times better than reported results for previous generation LYSO crystals

- Similar to liquid xenon energy resolution

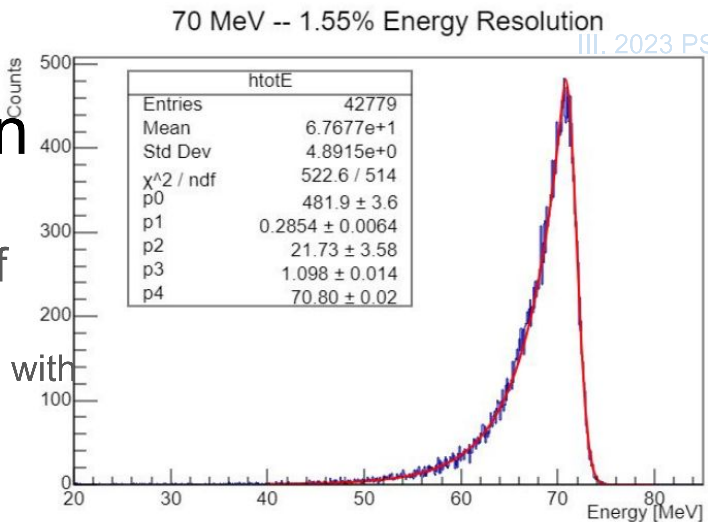

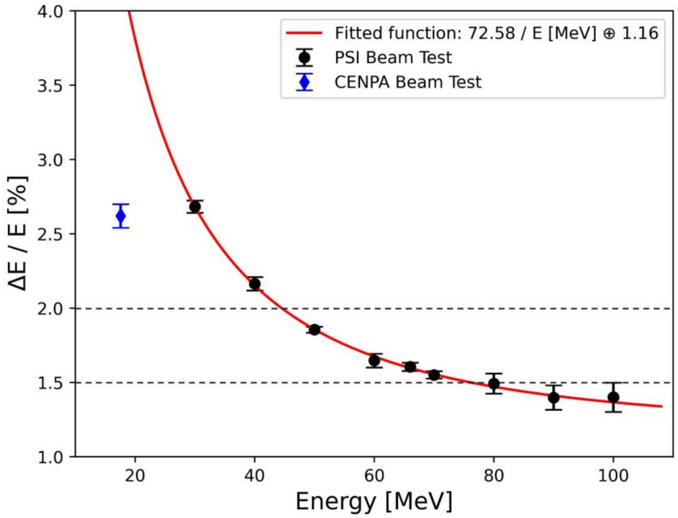

PIONEER DAQ Development

Development Overview

- DAQ work is split into a “hardware side” and “software side”
  - Cornell mostly handles the hardware side
  - UKY mostly handles the software side

- Hardware side goals:
  - Design a flexible system to handle real time data processing, digitizations, and triggers
  - Communication to software side over PCIe

- Software side goals:
  - Handle electronics readout and communication over PCIe
  - Handle data processing and compression

j.carlton@uky.edu

Proposed Framework

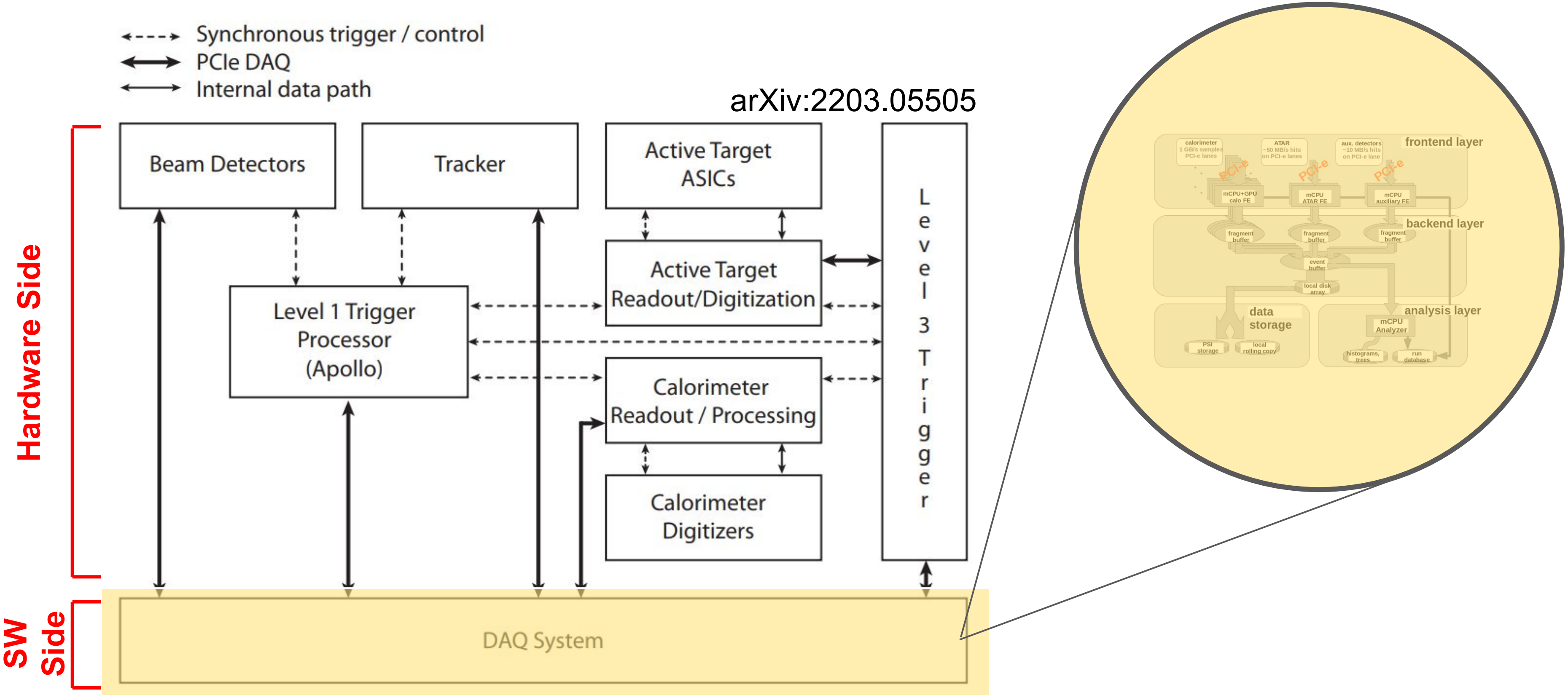

Proposed Framework

arXiv:2203.05505

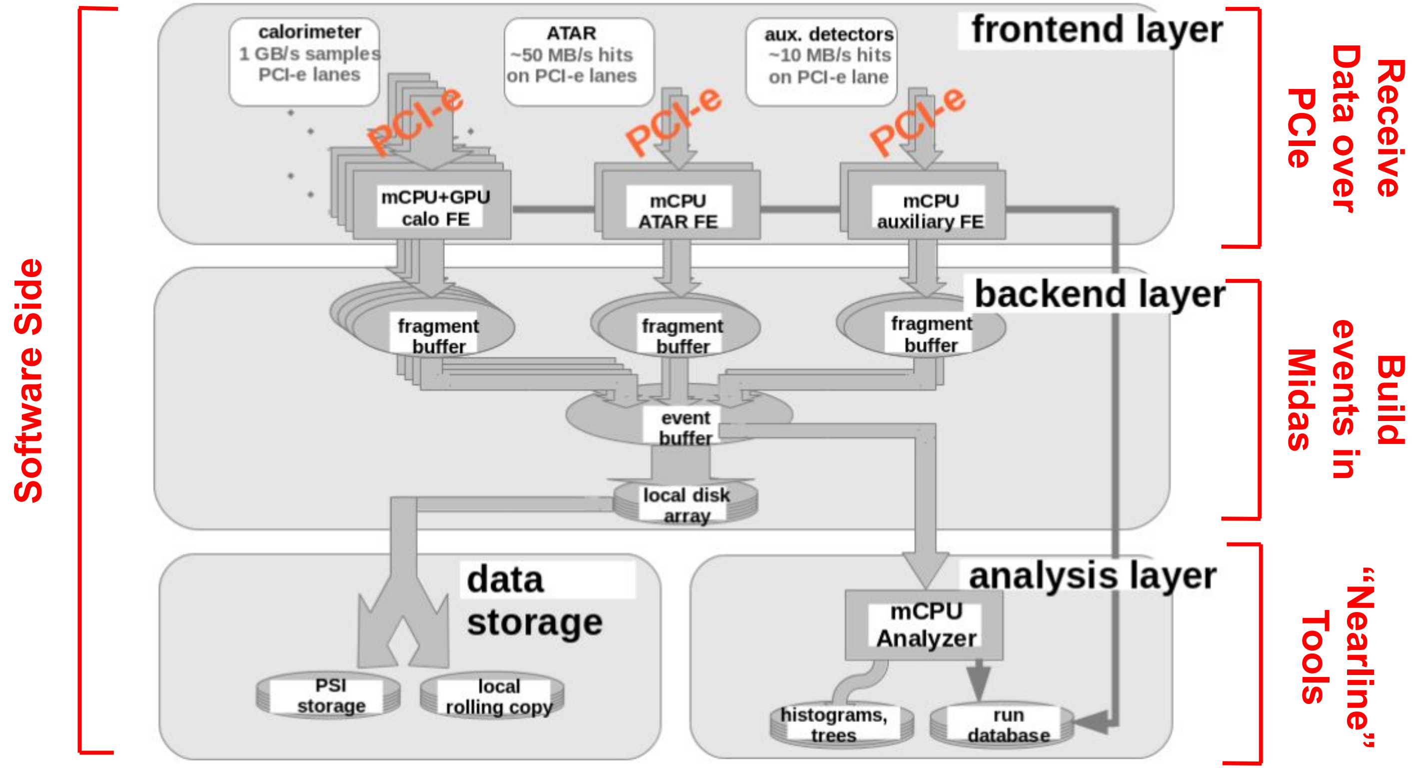

Proposed Experimental Hardware

- Using APOLLO system (no more µTCA crates)
- Data is moved using “Firefly” optical flyover system
  - 25 gb/s > 10gb/s links from g-2
- Data received by desktop through Firefly PCIe cards

Command Module (CU)

+

Service Module (BU)

=

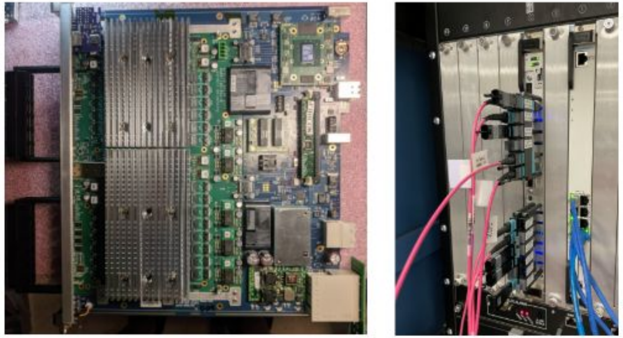

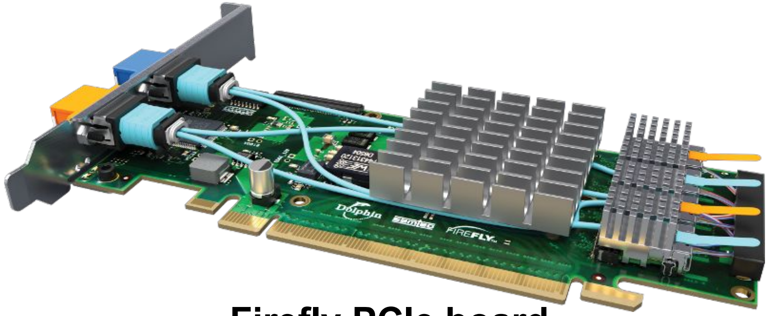

Firefly PCIe board

Mock Experimental Hardware - Our Development FPGA

- Using Nereid Development board
  - Kintex-7 FPGA
  - Data transfer over PCIe
  - Onboard RAM (data buffers)
  - FMC module input
- Why this board?
  - More learning resources
  - Has components to simulate real experimental hardware
- Limitations:
  - Only supports 5 GT/s (equivalent to PCIe 2)
  - Only 4 lanes (max throughput 2 GB/s)

Nereid K7 PCI Express FPGA Development Board

Mock Experimental Hardware - FPGA Firmware

- Using Xilinx intellectual property (IP) blocks in Vivado
  - IP blocks configured by development board settings
- Allows for direct memory access (DMA) transfer over PCIe between card and host

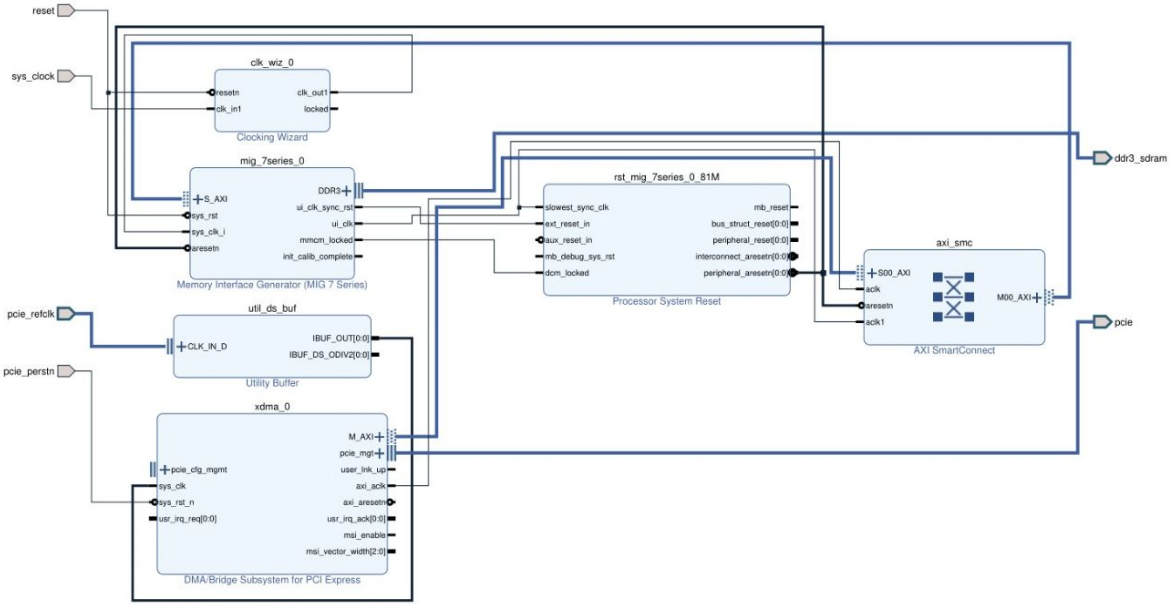

Block diagram for DMA transfer between board RAM and host (desktop) RAM

Data Rates Achieved

- More interested in read/Card-to-host (c2h) transfer rates
- Transfer rates are faster for larger data transfer sizes
- Using multiple channels, highest data throughput through midas was **1GB/s**
- This number is largely limited by the Nereid development board's hardware

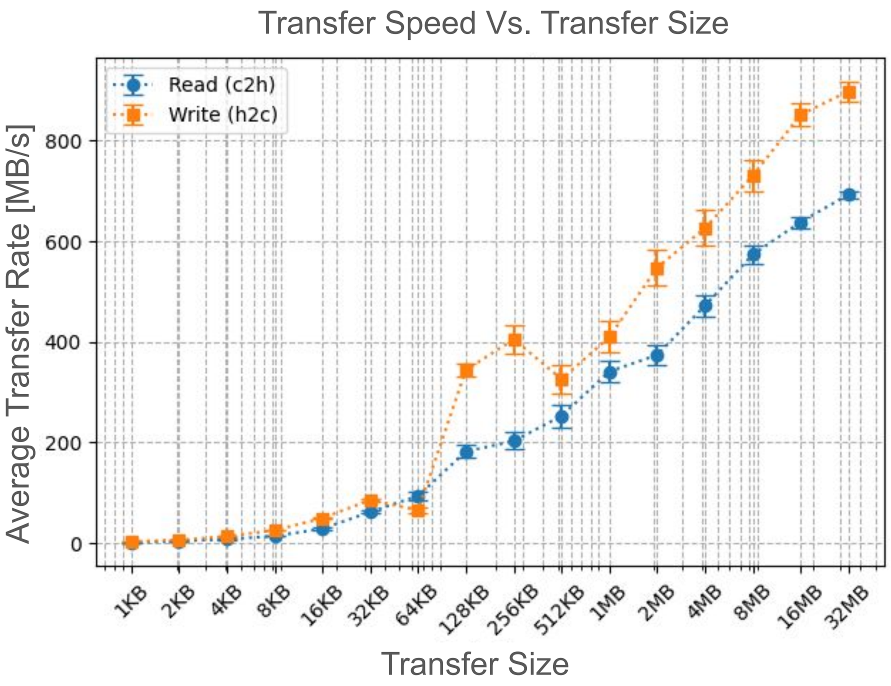

DMA transfer rate vs transfer size over one channel

Template Fitting - Example

- Can construct a continuous template for our traces $T(t)$
- Can fit traces using template: $f(t) = A \cdot T(t - t_0) + B$
- Storing unfit traces takes ~12 bits per ADC sample
- Storing residuals takes ~4 bits per ADC sample
- By fitting, we can compress the data by a **factor of ~3**

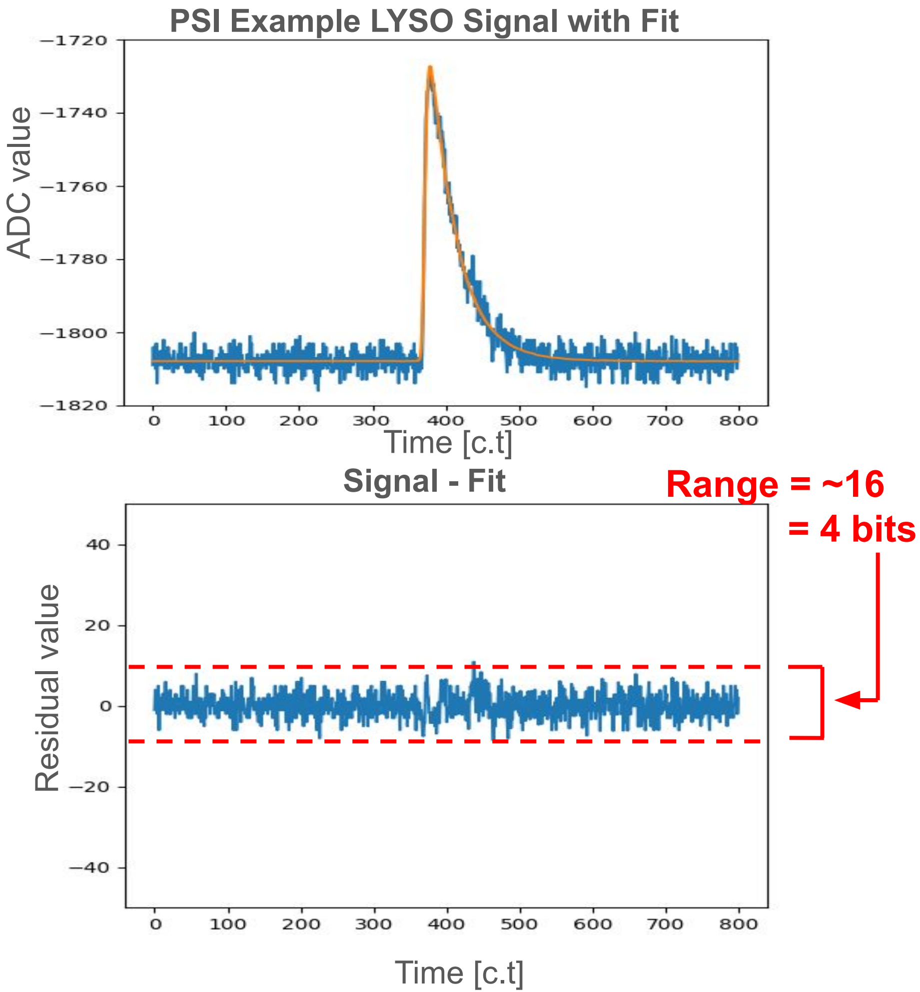

Template Fitting - Applied

- Data from PSI test beam
- Each vertical slice corresponds to pdf $p_i(x_i)$
- Template fit drastically reduces spread of data

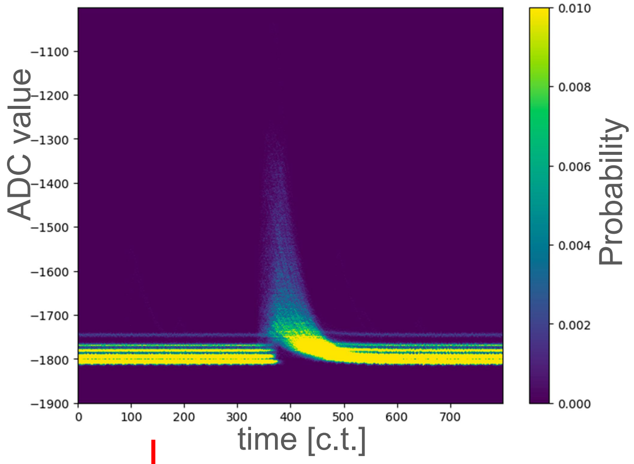

Template fitting

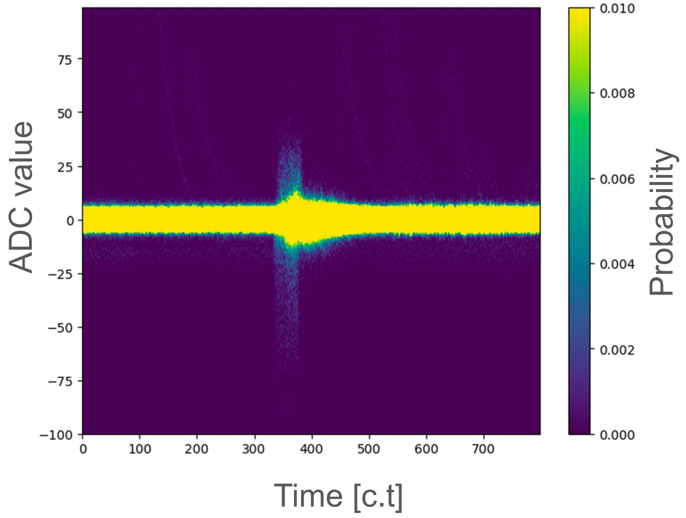

Theoretical Best Compression

- For lossless compression, the best possible compression rate is the entropy rate
- Entropy rate of pedestal part of signal is **3.4 bits per ADC sample**
  - A perfect fit would reduce signal to pedestal noise
- Best possible data storage rate 3.5 GB/s → **~1 GB/s**
  - Assumes similar noise to PSI test beam data
- Realistically the data storage rate depends how good our fit is
  - Assuming entropy rate of ~5 bits/sample 3.5 GB/s → ~1.5 GB/s

Entropy Rate Formula

$$H(X_i) = \sum_{\text{traces}} p(X_i) \log_2 (p(X_i))$$

$$X_i \equiv \text{Random variable for } i^{\text{th}} \text{ ADC sample}$$

Entropy Rate of PSI Test Beam Data After Fitting

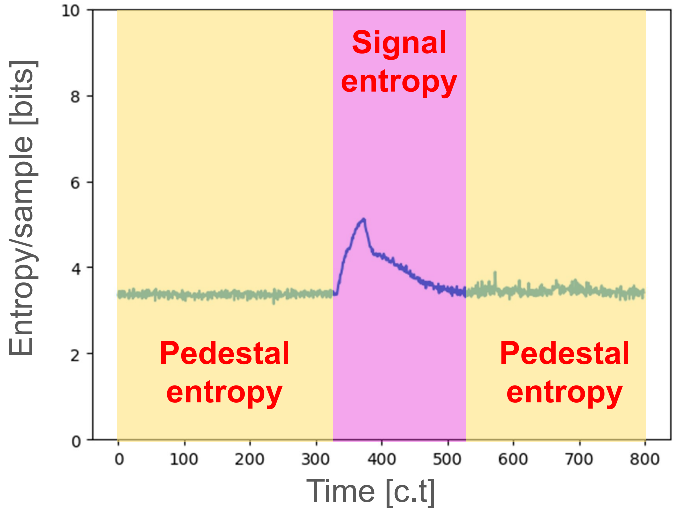

Current and Future Work

ATAR Teststand DAQ (Naludaq)

- Integrate Nalu's HDSoC digitizer output with MIDAS for synchronized, multi-detector event construction
  - Also utilize existing custom MIDAS-linked software
- Use Nalu's Python library for integration
  - Current readout via UART interface
  - Incorporate Nalu library into MIDAS frontend

Nexys A7 Video Board with Nalu's HDSoC Digitizer Attached as an FMC module

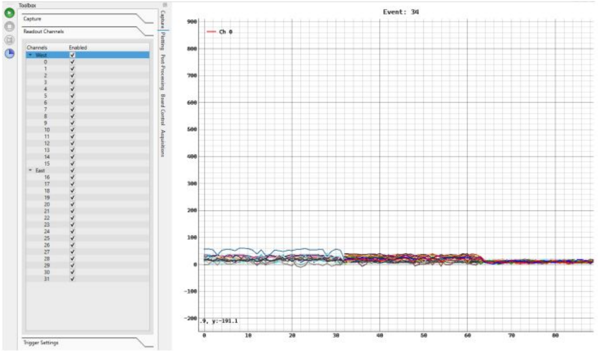

NaluScope Program Screenshot with Noise Traces

FPGA Firmware Additions

- Added MicroBlaze IP Block
- Allows the FPGA to run C++ code to edit onboard DDR3 RAM
  - Can code data generation simulators

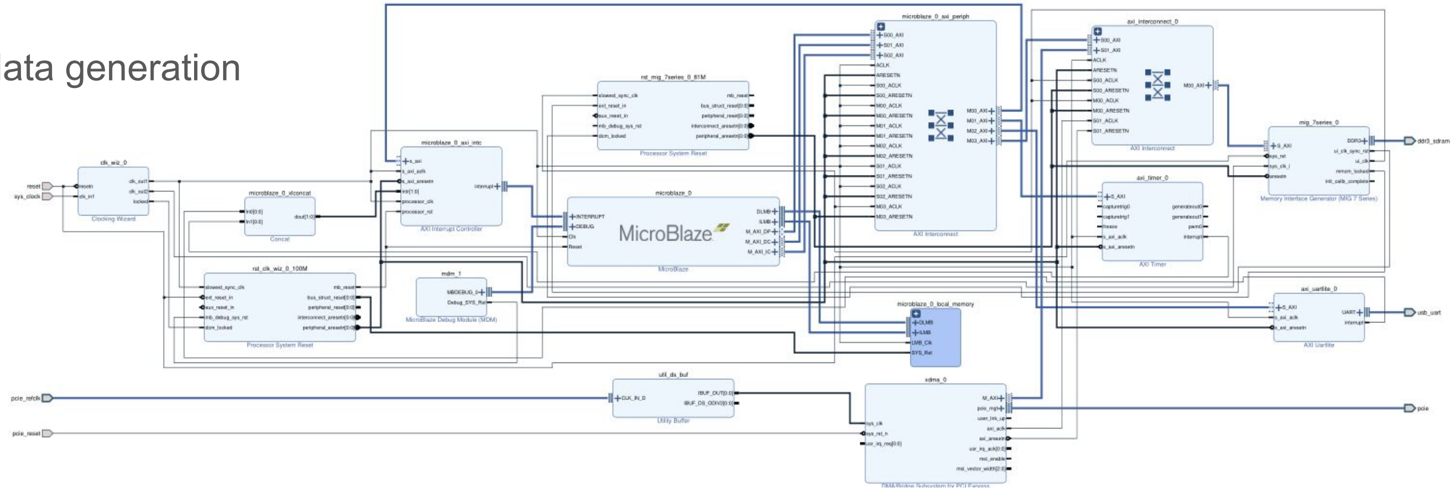

Block diagram for PCIe DMA transfer with microblaze

Generalizing and Optimizing Software

- Write modular software
  - Will make experiment DAQ code much more manageable in the future
- Optimize and adjust readout, compression, and other libraries (as needed)
- Write simple and scalable midas frontends
  - Implement libraries above

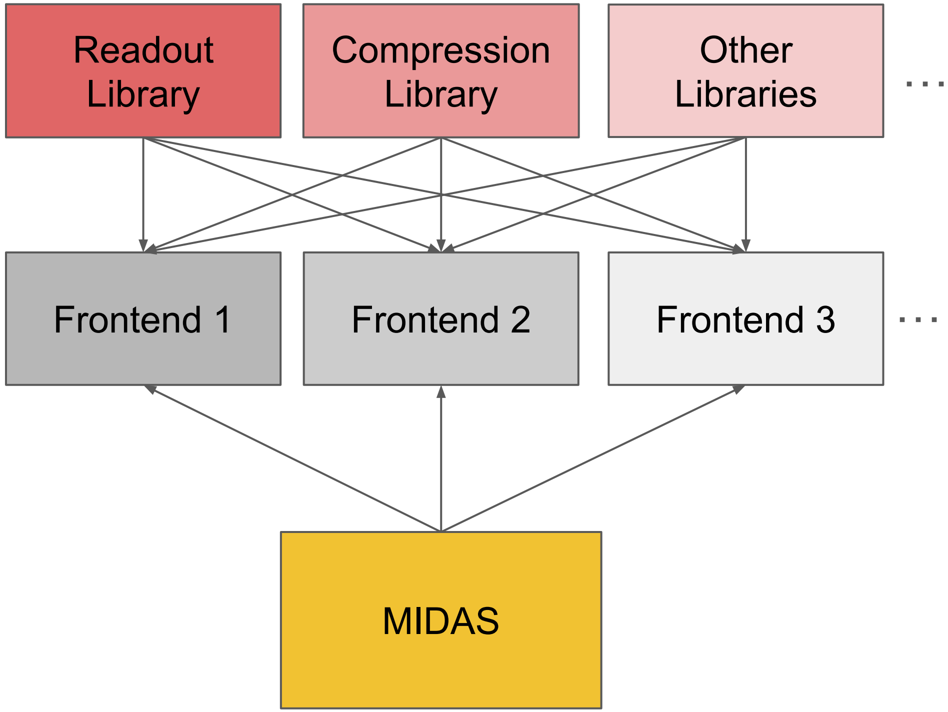

Dependency Diagram

PIONEER Demonstrator

- "Full" experiment demonstrator
- Prototypes for all detectors
  - Small number of ATAR Layers (16 layers)
  - Small spherical segment of tapered LYSO crystals (12 crystals)
  - Some spherical "shell" segment of tracker
- DAQ handles event construction

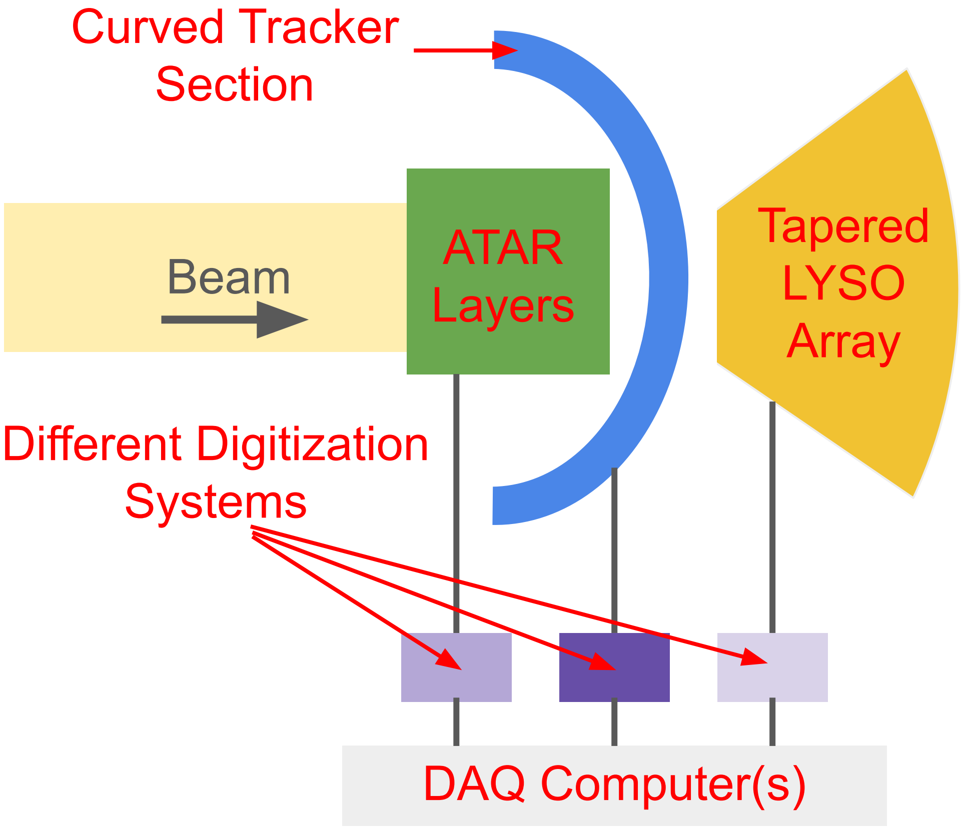

j.carlton@uky.edu

Auxiliary Slides

j.carlton@uky.edu

Background Physics

Citation: Wikipedia
(https://en.wikipedia.org/wiki/Pion)

j.carlton@uky.edu

Common Pion Decay Channels

[highlighted box] = Most Common

Leptonic Decay

- $\pi^+ \rightarrow e^+ + \nu_e$
- $\pi^- \rightarrow e^- + \overline{\nu}_e$
- $\pi^+ \rightarrow \mu^+ + \nu_\mu$ (most common)
- $\pi^- \rightarrow \mu^- + \overline{\nu}_\mu$ (most common)

Beta Decay

- $\pi^+ \rightarrow \pi^0 + e^+ + \nu_e$
- $\pi^- \rightarrow \pi^0 + e^- + \overline{\nu}_e$

Photon Decay

- $\pi^0 \rightarrow \gamma + \gamma$ (most common)

Dalitz Decay

- $\pi^0 \rightarrow \gamma + e^- + e^+$

Double-Dalitz Decay

- $\pi^0 \rightarrow e^- + e^+ + e^- + e^+$

Electrons

- $\pi^0 \rightarrow e^- + e^+$

[Note: Dalitz Decays are like photon decays, except the photon(s) are virtual and immediately decay into electron/positron pairs]

j.carlton@uky.edu

Naive Pion Decay, 2-body decay

- Without getting into details of QCD, we can treat this as a 3 particle decay
- We can use Fermi's golden rule:

$$d\Gamma = |\mathcal{M}|^2 \cdot \frac{1}{2\hbar m_a} \cdot \left[\frac{c d^3 \mathbf{p}_b^2}{(2\pi)^3 2E_b} \cdot \frac{c d^3 \mathbf{p}_c^2}{(2\pi)^3 2E_c} \right] \cdot (2\pi)^4 \delta^4 (p_a - p_b - p_c)$$

- After integration in the COM frame we find:

$$\Gamma = \frac{|\mathbf{p}|}{8\pi\hbar m_a^2 c} |\mathcal{M}|^2$$
$$\text{where } \mathbf{p} = \mathbf{p}_b = -\mathbf{p}_c$$

- $\longrightarrow \Gamma \propto$ p (not correct)
  - Details hidden in matrix element

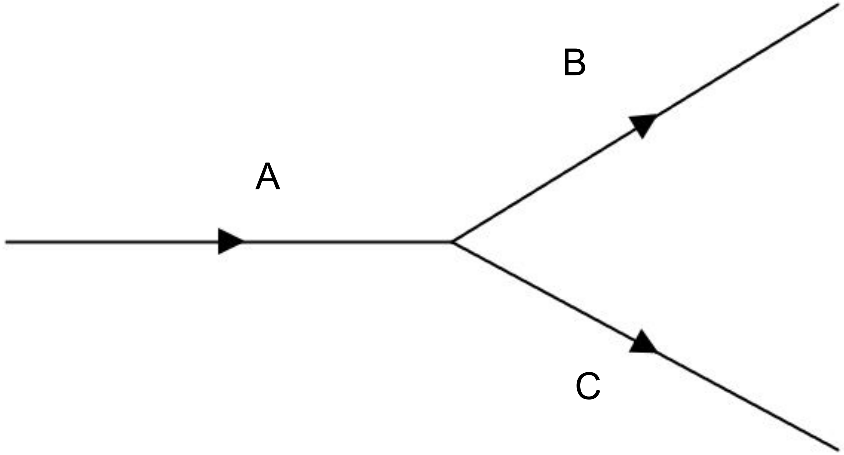

 j.carlton@uky.edu

Why Massless → Chirality States ~ Helicity States

- Massless → moves at c
- Moves at c → cannot reverse particle direction with Lorentz boost → helicity is Lorentz Invariant
- Chirality is a property of a particle, always Lorentz invariant! → helicity and chirality agree in direction in all inertial reference frames

$$(\gamma^\mu p_\mu - m)u(p) = 0$$ [Dirac Equation]

$$\Longrightarrow \begin{pmatrix} -mI_{2\times 2} & \sigma\cdot p \\ \bar{\sigma}\cdot p & -mI_{2\times 2} \end{pmatrix} \begin{pmatrix} u_L \\ u_R \end{pmatrix} = 0$$

[Chiral States]

$$\Longrightarrow \begin{cases} (\sigma\cdot p)u_R - mu_L = 0 \\ (\bar{\sigma}\cdot p)u_L - mu_R = 0 \end{cases}$$

$$m \to 0 \;\Longrightarrow \begin{cases} (p_0 - \boldsymbol{\sigma}\cdot\mathbf{p})u_R = 0 \\ (p_0 + \boldsymbol{\sigma}\cdot\mathbf{p})u_L = 0 \end{cases}$$

$$\Longrightarrow \begin{cases} \frac{\boldsymbol{\sigma}\cdot\mathbf{p}}{|\mathbf{p}|}u_R = u_R \\ \frac{\boldsymbol{\sigma}\cdot\mathbf{p}}{|\mathbf{p}|}u_L = -u_L \end{cases}$$

$$\hat{h} = \frac{\mathbf{S}\cdot\mathbf{p}}{|\mathbf{p}|} = \frac{1}{2}\frac{\boldsymbol{\sigma}\cdot\mathbf{p}}{|\mathbf{p}|}$$ [Helicity operator]

$$\Longrightarrow \begin{cases} \hat{h}u_R = \frac{1}{2}u_R \\ \hat{h}u_L = -\frac{1}{2}u_L \end{cases}$$ [Chiral states are eigenstates of helicity operator]

 j.carlton@uky.edu

LH (negative) helicity spinor to chiral components

An negative helicity antiparticle can be written as

$$v_{\downarrow} = \sqrt{E+m} \begin{pmatrix} \frac{|\mathbf{p}|}{E+m}\cos(\frac{\theta}{2}) \\ \frac{|\mathbf{p}|}{E+m}\sin(\frac{\theta}{2})e^{i\phi} \\ \cos(\frac{\theta}{2}) \\ \sin(\frac{\theta}{2})e^{i\phi} \end{pmatrix}$$

Where (θ,φ) define the direction of the momentum. Without loss of generality, assume the momentum is in the z direction

$$v_{\downarrow} = \sqrt{E+m} \begin{pmatrix} \frac{|\mathbf{p}|}{E+m} \\ \frac{|\mathbf{p}|}{E+m} \\ 1 \\ 1 \end{pmatrix} \equiv A \begin{pmatrix} \tau\xi_R \\ \xi_R \end{pmatrix}$$

j.carlton@uky.edu

LH (negative) helicity spinor to chiral components

We can use the chiral projection operations to project this helicity state to chiral state

$$v_\downarrow = P_L v_\downarrow + P_R v_\downarrow$$

$$P_R = \frac{I_{4\times4} + \gamma^5}{2} = \begin{pmatrix} I_{2\times2} & I_{2\times2} \\ I_{2\times2} & I_{2\times2} \end{pmatrix}$$

$$P_L = \frac{I_{4\times4} - \gamma^5}{2} = \begin{pmatrix} I_{2\times2} & -I_{2\times2} \\ -I_{2\times2} & I_{2\times2} \end{pmatrix}$$

$$v_\downarrow = \frac{A}{2}\left[(1-\tau)\begin{pmatrix} -\xi_R \\ \xi_R \end{pmatrix} + (1+\tau)\begin{pmatrix} \xi_R \\ \xi_R \end{pmatrix}\right] \equiv \frac{A}{2}(1-\tau)v_R - \frac{A}{2}(1+\tau)v_L$$

Where the left and right chiral anti-particle states are defined by

$$P_L v_R = v_R \text{ and } P_R v_L = v_L$$

 j.carlton@uky.edu

LH (negative) helicity spinor to chiral components

Looking at the chiral projection of a negative helicity state, we can see in general there are left **and** right chiral components, so the weak force **can** act on a LH (negative) anti-particle helicity state

$$v_{\downarrow} = \frac{A}{2}\left[\left(1 - \frac{p}{E+m}\right)v_R - \left(1 + \frac{p}{E+m}\right)v_L\right]$$

It should also be clear as m→0, the LH (negative) helicity state coincides with the LH chiral state.

This means W boson decay to two massless leptons is forbidden! One of the particles must have the wrong chirality, and thus low mass decays will be suppressed.

j.carlton@uky.edu

Matrix Element Details

$$\mathcal{M}_{fi} = \left[\frac{g_W}{\sqrt{2}}\frac{1}{2}f_\pi p_\pi^\alpha\right]\cdot\left[\frac{g_{\alpha\beta}}{m_W^2}\right]\cdot\left[\frac{g_W}{\sqrt{2}}g_l\bar{u}(p_l)\gamma^\beta\frac{1}{2}(1-\gamma^5)v(p_\nu)\right]$$

Move to pion rest frame so only $p^0 = m_\pi$ remains:

$$\mathcal{M}_{fi} = \frac{g_W^2 f_\pi g_l}{4m_W^2}m_\pi\bar{u}(p_l)\gamma^0\frac{1}{2}(1-\gamma^5)v(p_\nu)$$

Using the identity: $\bar{u}(p_l)\gamma^0 = u^\dagger(p_l)\gamma^0\gamma^0 = u^\dagger(p_l)I_{4\times 4} = u^\dagger(p_l)$

$$\mathcal{M}_{fi} = \frac{g_W^2 f_\pi g_l}{4m_W^2}m_\pi u^\dagger(p_l)\frac{1}{2}(1-\gamma^5)v(p_\nu)$$

j.carlton@uky.edu

Matrix Element Details

For a neutrino m << E so helicity eigenstate is essentially the chiral eigenstate:

$$\frac{1}{2}(1-\gamma^5)v(p_\nu) = v_\uparrow(p_\nu) \implies \mathcal{M}_{fi} = \frac{g_W^2 f_\pi g_l}{4m_W^2} m_\pi u^\dagger(p_l) v_\uparrow(p_\nu)$$

By letting the lepton go in the z-direction we can write:

$$u(p_l) = u_\uparrow(p_l) + u_\downarrow(p_l) = \sqrt{E_l + m_l}\left[\begin{pmatrix} 1 \\ 0 \\ \frac{p}{E_l+m_l} \\ 0 \end{pmatrix} + \begin{pmatrix} 0 \\ 1 \\ 0 \\ \frac{-p}{E_l+m_l} \end{pmatrix}\right] \quad \text{and} \quad v(p_\mu) = v_\uparrow(p_\mu) = \sqrt{p}\begin{pmatrix} 1 \\ 0 \\ -1 \\ 0 \end{pmatrix}$$

Negative helicity lepton down state disappears when "dotted" with the neutrino state:

$$\mathcal{M}_{fi} = \frac{g_W^2 f_\pi g_l}{4m_W^2} m_\pi \sqrt{E_l + m_l}\sqrt{p}\left(1 - \frac{p}{E_l + m_l}\right)$$

j.carlton@uky.edu

Matrix Element Details

$$\mathcal{M}_{fi} = \frac{g_W^2 f_\pi g_l}{4m_W^2} m_\pi \sqrt{E_l + m_l}\sqrt{p}\left(1 - \frac{p}{E_l + m_l}\right)$$

We can re-write E_l and p in the limit where the neutrino mass is zero:

$$E_l = \frac{m_\pi^2 + m_l^2}{2m_\pi} \text{ and } p_l = \frac{m_\pi^2 - m_l^2}{2m_\pi}$$

$$\implies \mathcal{M}_{fi} = \frac{g_W^2 f_\pi g_l}{4m_W^2} m_\pi \cdot \frac{m_\pi + m_l}{\sqrt{2m_\pi}} \cdot \left(\frac{m_\pi^2 - m_l^2}{2m_\pi}\right)^{\frac{1}{2}} \cdot \frac{2m_l}{m_\pi + m_l}$$

$$\implies \mathcal{M}_{fi} = \frac{g_W^2 f_\pi g_l}{4m_W^2} \cdot m_l (m_\pi^2 - m_l^2)^{\frac{1}{2}}$$

j.carlton@uky.edu

Lepton Universality

$$\text{Note: } x^2 = 1 + 2(x-1) + \mathcal{O}(x^2)$$

$$\text{Let: } \left(\frac{g_e}{g_\mu}\right) \equiv (1 + \Delta_{\frac{g_e}{g_\mu}}) \equiv x$$

$$R_{e/\mu} = \frac{\Gamma(\pi^- \to e^- \bar{\nu}_e)}{\Gamma(\pi^- \to \mu^- \bar{\nu}_\mu)} \approx (1+2\Delta_{\frac{g_e}{g_\mu}}) \left[\frac{m_e(m_\pi^2 - m_e^2)}{m_\mu(m_\pi^2 - m_\mu^2)}\right]^2$$

$$\text{Let: } \Delta R_{e/\mu} = R_{e/\mu} - (R_{e/\mu})_{\text{theory}}$$

$$\boxed{\frac{\Delta R_{e/\mu}}{(R_{e/\mu})_{\text{theory}}} = 2\Delta_{\frac{g_e}{g_\mu}}} \implies$$

Small discrepency in g_e/g_μ and 1 can cause twice as big discrepency in measured $R_{e/\mu}$ and theory $R_{e/\mu}$

j.carlton@uky.edu

Another Test for Lepton Universality

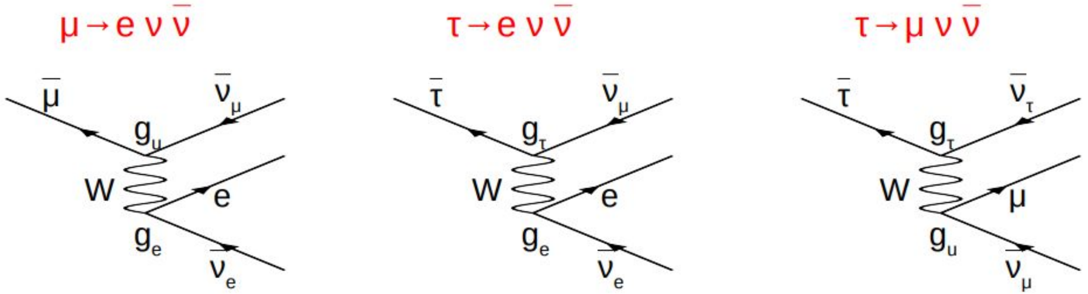

Fermi constant, $G_F = g^2 / 4\sqrt{2}M_W^{\ 2}$

$G_{\mu e}$ = 1.166 378 7(6)x10^{-5} GeV^{-2} (0.5 ppm)

$G_{\tau\mu}$ = 1.1665(28)x10^{-5} GeV^{-2} (0.2%)

$G_{\tau e}$ = 1.1665(28) x 10^{-5} GeV^{-2} (0.2%)

weak coupling, g

$g_e : g_\mu : g_\tau$ 1 : 1.0011(24) : 1.0006(24)

j.carlton@uky.edu

CKM Unitary Test

arXiv:2203.05505

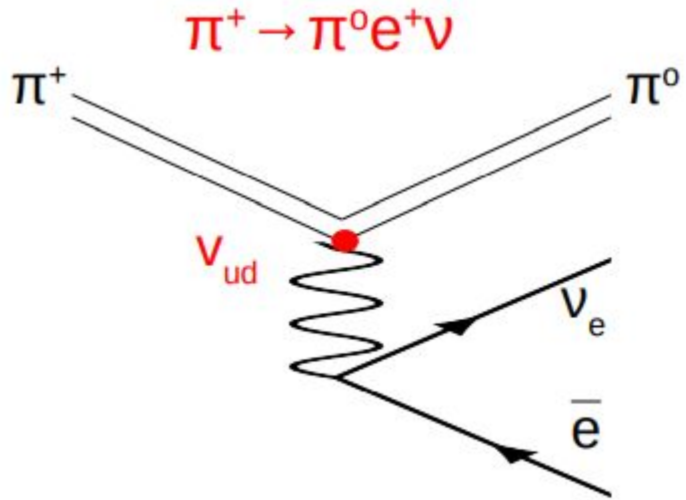

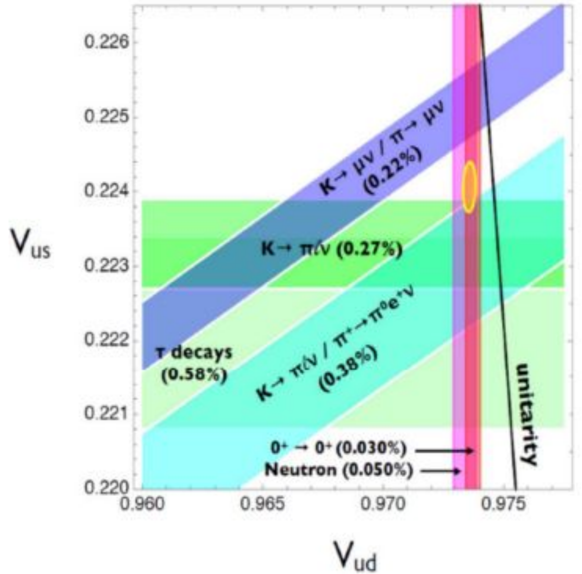

- Pion beta decay gives a precision measurement of V_{ud}
- These decays are lower rate than $\pi \rightarrow e\nu_e$ and $\pi \rightarrow \mu\nu_\mu$
- Experimental measurements do not agree

Citations: A measurement of the scintillation decay time constant of nuclear recoils in liquid xenon with the XMASS-I detector, XMASS collab, arxiv 1809.05988
Scintillation yield of liquid xenon at room temperature , XMASS collab, arxiv 0803.2888
Berkeley Nucleonics (https://www.berkeleynucleonics.com/nai-sodium-iodide)

j.carlton@uky.edu

Some Information about LXe and NaI

- LXe has singlet and triplet state decay constants:
  - $\tau_S = 4.3 \pm 0.6$ ns
  - $\tau_T = 26.9^{+0.7}_{-1.1}$ ns
- LXe light yield:
  - ~29 photons/keV at room temp
- NaI decay constant:
  - ~ 250 ns
- NaI light yield:
  - 38 photons/keV at room temp

Scintillation from excited Xe (Xe*):

$$\mathrm{Xe}^* + \mathrm{Xe} + \mathrm{Xe} \rightarrow \mathrm{Xe}_2^* + \mathrm{Xe}\,,$$
$$\mathrm{Xe}_2^* \rightarrow 2\mathrm{Xe} + h\nu\,.$$

Scintillation from ionized Xe (Xe⁺):

$$\mathrm{Xe}^+ + \mathrm{Xe} \rightarrow \mathrm{Xe}_2^+\,,$$
$$\mathrm{Xe}_2^+ + e^- \rightarrow \mathrm{Xe}^{**} + \mathrm{Xe}\,,$$
$$\mathrm{Xe}^{**} \rightarrow \mathrm{Xe}^* + heat\,,$$
$$\mathrm{Xe}^* + \mathrm{Xe} + \mathrm{Xe} \rightarrow \mathrm{Xe}_2^* + \mathrm{Xe}\,,$$
$$\mathrm{Xe}_2^* \rightarrow 2\mathrm{Xe} + h\nu\,.$$

j.carlton@uky.edu

PEN

- Similar to PIENU
  - Segmented
  - Better timing

- Many channels of pure CSI
  - 240 channels

- Active target

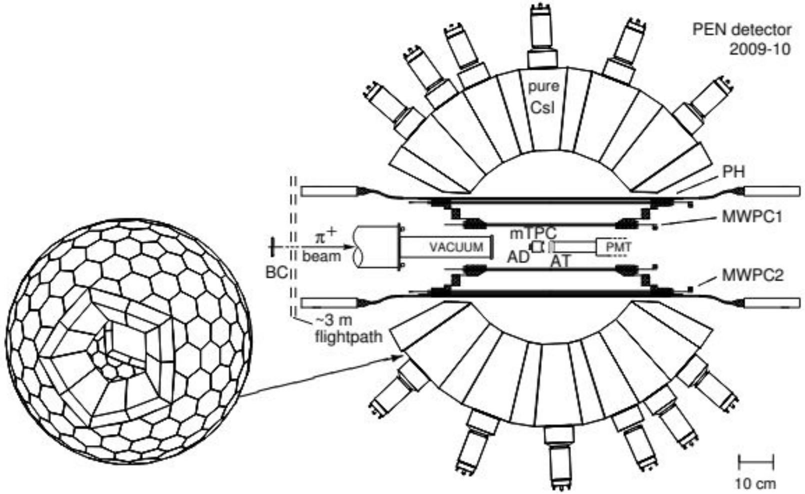

Citation: PSI Ring Cyclotron Proposal R-22-01.1 PIONEER: Studies of Rare Pion Decays, PIONEER collab, (pg. 19 arxiv: 2203.01981)

j.carlton@uky.edu

More ATAR details

- Pion and muon decays deposit energy into ATAR
- Allow event types to be distinguished
- Muons decaying in flight can boost positron energy past 53 MeV (big issue!)
  - ATAR can give information to rebuild event, and correctly classify a muon decay

arxiv: 2203.01981

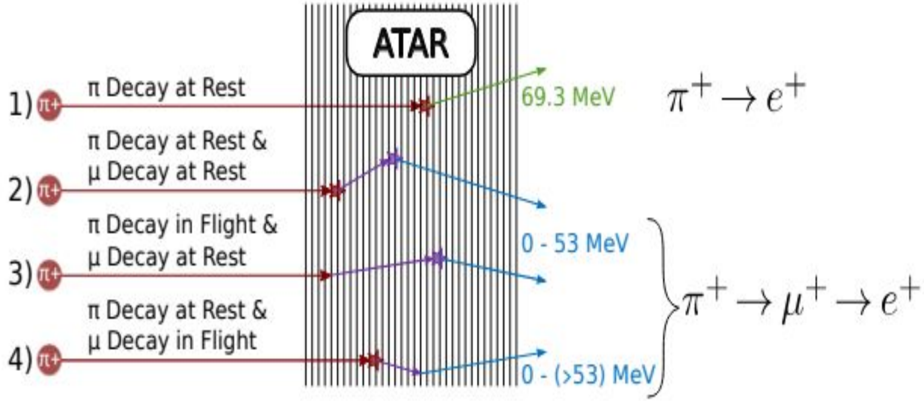

Citations: PIONeer A next-generation rare pion decay experiment, David Hertzog, (https://pioneer.npl.washington.edu/docdb/0002/000281/001/PIONEER%20Orientation%20and%20Status%20June%202024.pdf)

j.carlton@uky.edu

Another Calorimeter 3D Render (Liquid Xenon)

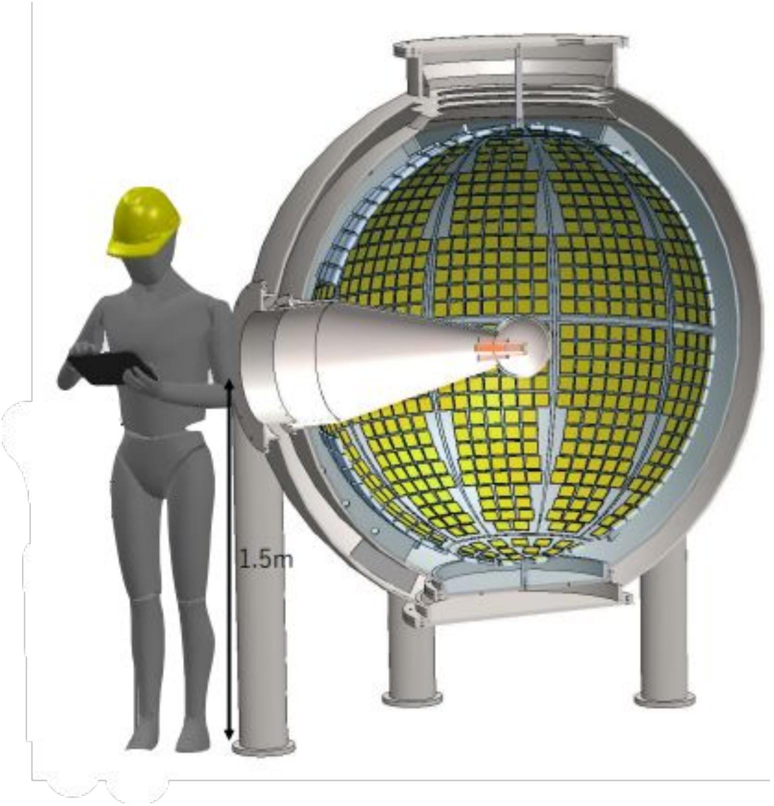

j.carlton@uky.edu

Electronics and Data Rates

j.carlton@uky.edu

Initialism Cheatsheet

Initialism	Meaning	Example
10GbE	10 Gigabit Ethernet	
FPGA	Field Programmable Gate Array	
FMC	FPGA Mezzanine Card	FC7 SFP Interface
CPU	Central Processing Unit	Intel Core i7-12700K
GPU	Graphics Processing Unit	NVIDIA A5000
µTCA (uTCA)	Micro Telecommunications Computing Architecture	
WFD	Waveform Digitizer	WFD5
FC	Flexible Controller	FC7
AMC	Advanced Mezzanine Card	AMC13 (also FC7 and WFD5)
MCH	MicroTCA Carrier Hub	
DDR	Double Data Rate	DDR3, DDR4 (RAM)
PCIe	Peripheral Component Interconnect Express	PCIe2, PCIe3, ...
TTC	Timing, Trigger, and Control	
UART	Universal Asynchronous Receiver-Transmitter	

j.carlton@uky.edu

Hardware - Conceptual Diagram

- Differential signal into WFD5 (Waveform Digitizer)
- Trigger signal into FC7 (Flexible Controller)
- AMC13 (Advanced Mezzanine Card) gathers data, sends over 10GbE (10 Gigabit Ethernet) to desktop
- MCH (MicroTCA Carrier Hub) facilitates Desktop↔Crate communication over 1GbE
- Desktop CPU handles event processing
- Meinberg gives trigger timestamp to computer

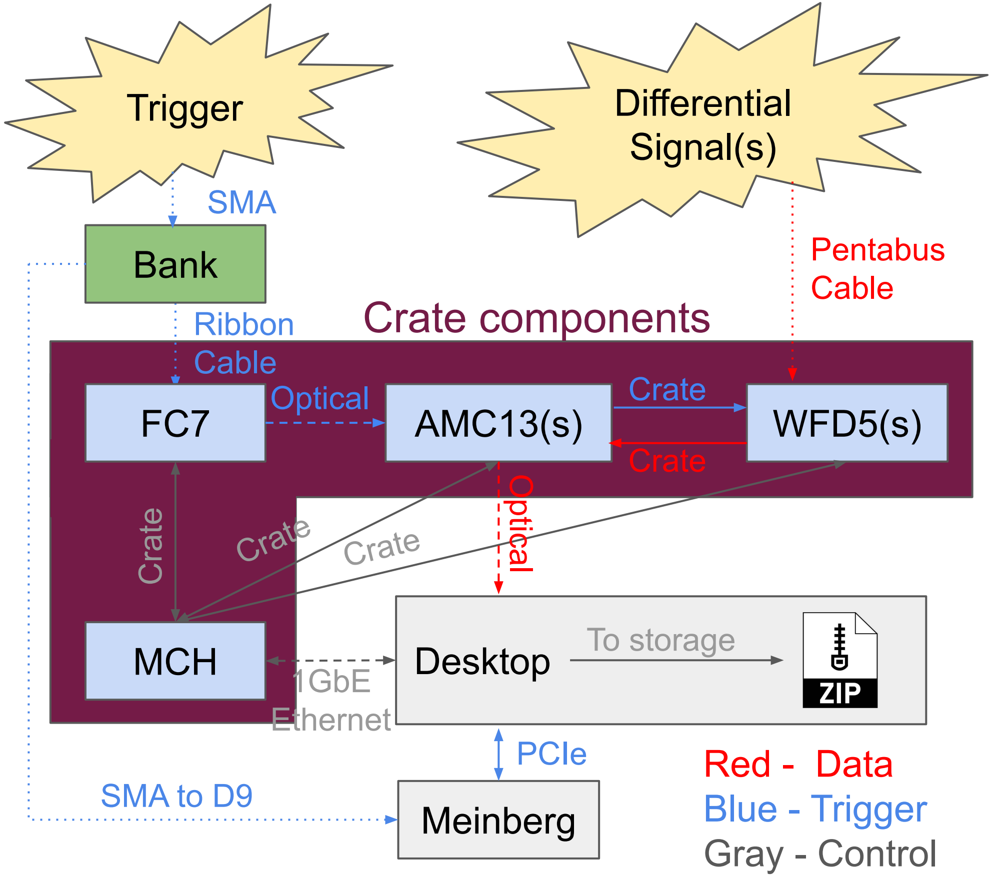

j.carlton@uky.edu

Hardware - Unlabeled Picture

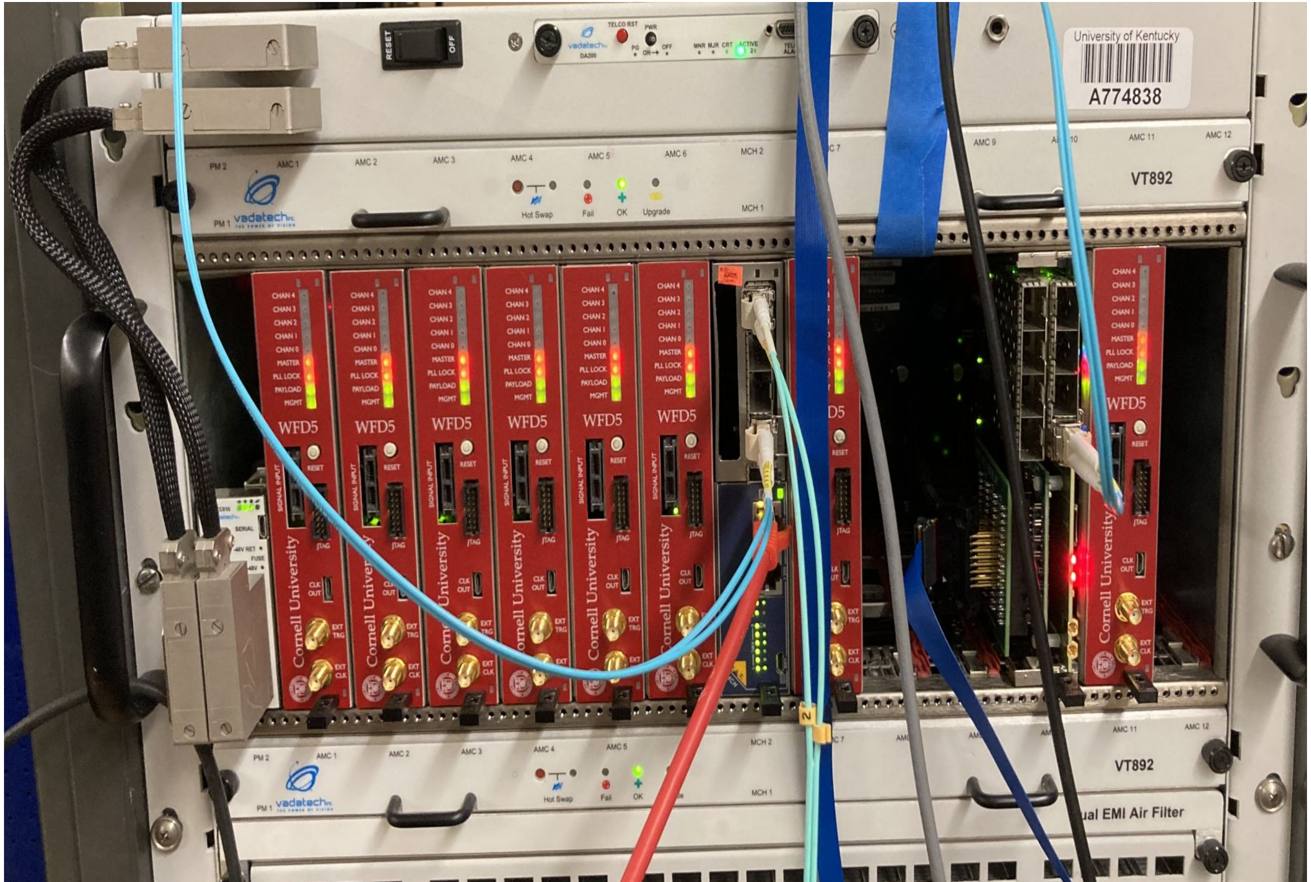

Citation: DAQ electronics status, Lawrence Gibbons (Slide 1)
https://pioneer.npl.washington.edu/cgi-bin/private/ShowDocument?docid=245

j.carlton@uky.edu

PIONEER DAQ (in a nascent state)

- PIONEER DAQ
  - In nascent development state
  - Design catered to PIONEER full experiment necessities

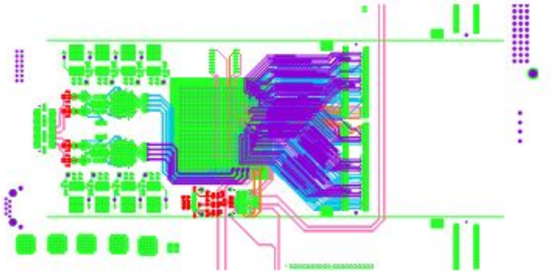

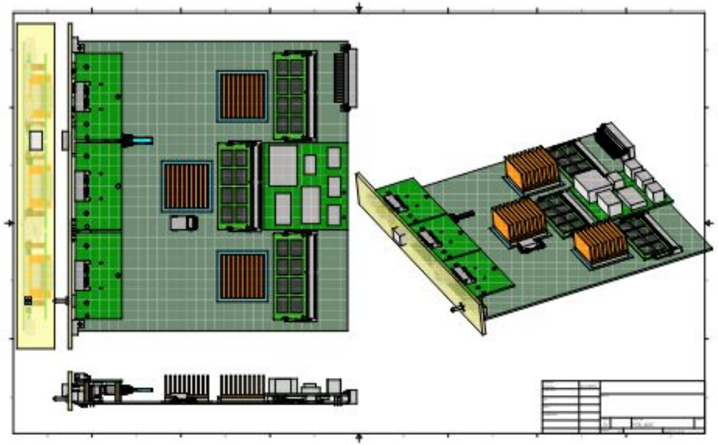

PIONEER ADC schematic drawings

j.carlton@uky.edu

“Older” PCIe DMA Transfer Rates are Better

- Transfer rates using block ram in a computer with an older OS (CentOS7)
- There is a leveling off effect at high transfer sizes
- XDMA driver by Xilinx seems to changes with kernel version, causing performance differences

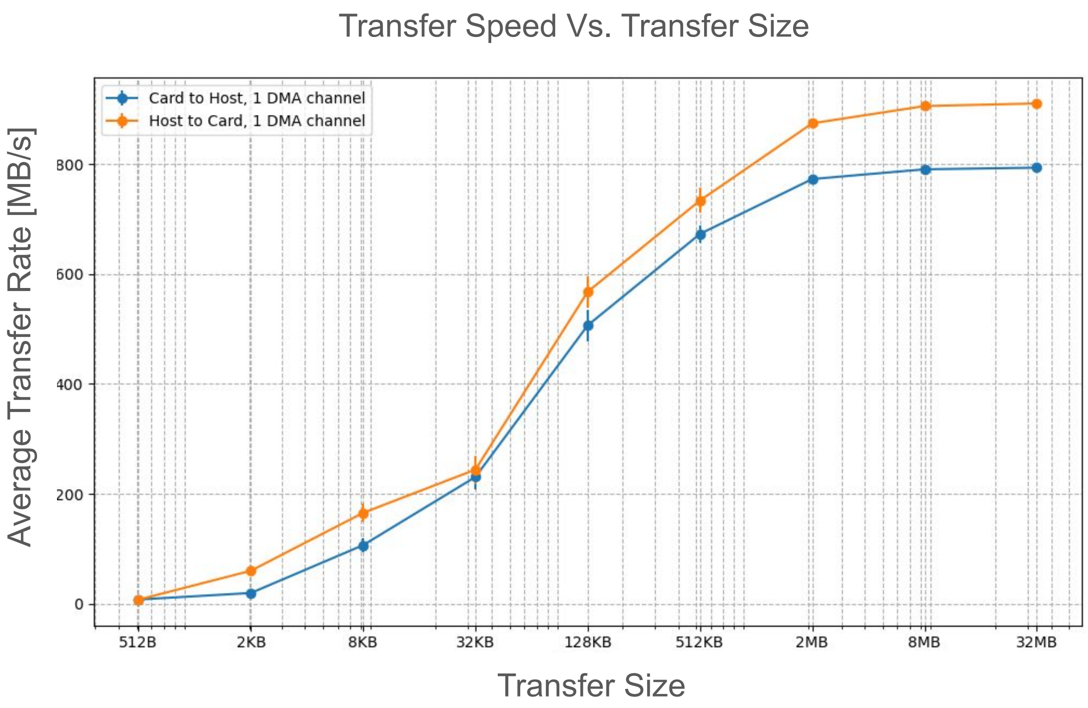

Citation: PSI Ring Cyclotron Proposal R-22-01.1 PIONEER: Studies of Rare Pion Decays, PIONEER collab (pg. 33)

j.carlton@uky.edu

Data Rates (CALO data rates LXe/LYSO dependant)

arXiv:2203.01981

triggers	prescale	range TR(ns)	rate (kHz)	CALO ΔT(ns)	CALO chan	CALO MB/s	ATAR digitizer ΔT(ns)	ATAR digitizer chan	ATAR digitizer MB/s	ATAR high thres chan	ATAR high thres MB/s
PI	1000	-300,700	0.3	200	1000	120	30	66	2.4	20	0.012
CaloH	1	-300,700	0.1	200	1000	40	30	66	0.8	20	0.004
TRACK	50	-300,700	3.4	200	1000	1360	30	66	27	20	0.014
PROMPT	1	2,32	5	200	1000	2000	30	66	40	20	0.2

- PIONEER DAQ expects data rate of ~**3.5GB/s**
- Considering running time, this is ~**35,000 TB/year**
- How do we compress this in real time?
    - Fit data, store fit parameters
    - Compress and store residuals, throw some out
    - Graphics Processing Units (GPUs) used for this operation

j.carlton@uky.edu

PSI Data

j.carlton@uky.edu

Contributions

- Repurposing g-2 DAQ Software
- Flexible Pipeline for Data Quality Monitor
- Beamtime “Live” DAQ Maintenance
- Onsite preliminary data analysis

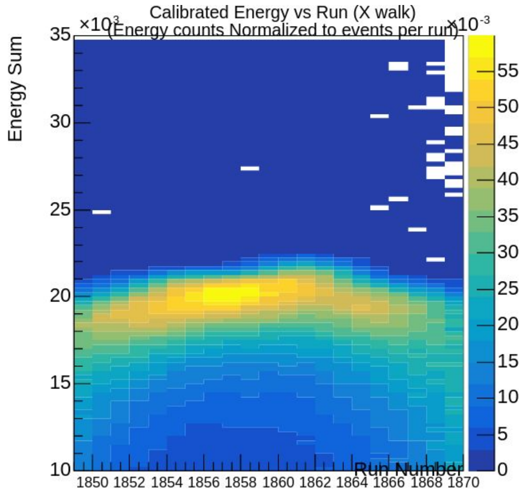

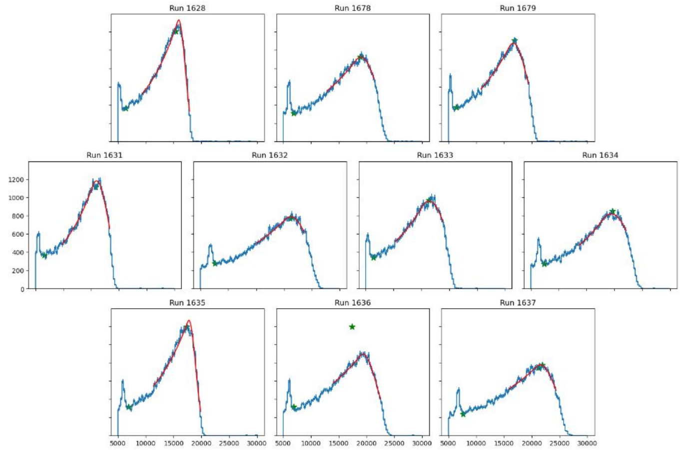

Examples of preliminary analysis work done at PSI

j.carlton@uky.edu

LYSO Information

- LYSO – lutetium–yttrium oxyorthosilicate
  - Lutetium (73%), Oxygen (18%), Silicon (6%), Yttrium (3%), and a Cerium scintillation dopant (~ 0%)
- Density = **7.4 g/cm^3**
- X_0 = **1.14 cm** = "Radiation length" = distance for an electron's energy to be reduced by a factor of 1/e
- R_M = **2.07 cm** = "Moliére radius" = radius of a cylinder containing on average 90% of the shower's energy deposition
- Light Yield = **30,000 photons/MeV**
- Scintillating decay time = **40 ns**

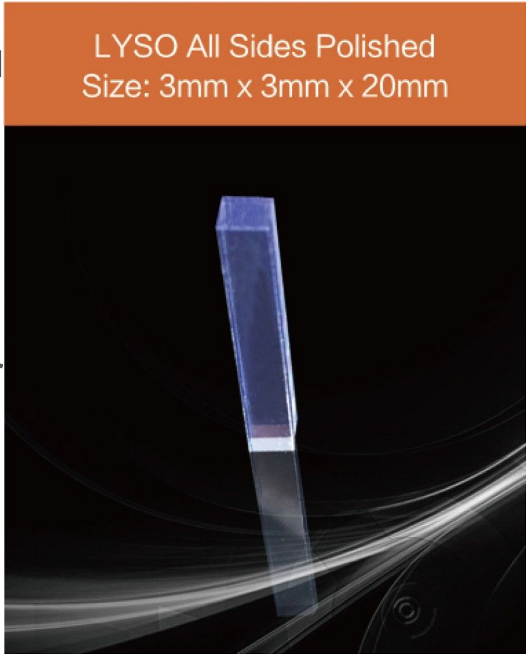

j.carlton@uky.edu

Energy Resolution Definition

- Energy resolution = ΔE/E
  - E is the peak energy
  - ΔE is the width of the peak
- Gaussian fit around the peak
  - a "crystal ball" fit is used here
  - Gaussian around center, x^{-n} on "sides" where n is a parameter
  - Gaussian parameter σ used for ΔE
- In this case, p4 = **E = 70.80 ± 0.02 MeV**
- p3 = **ΔE = 1.098 ± 0.014 MeV**
- ΔE/E = 0.0155 = 1.55%

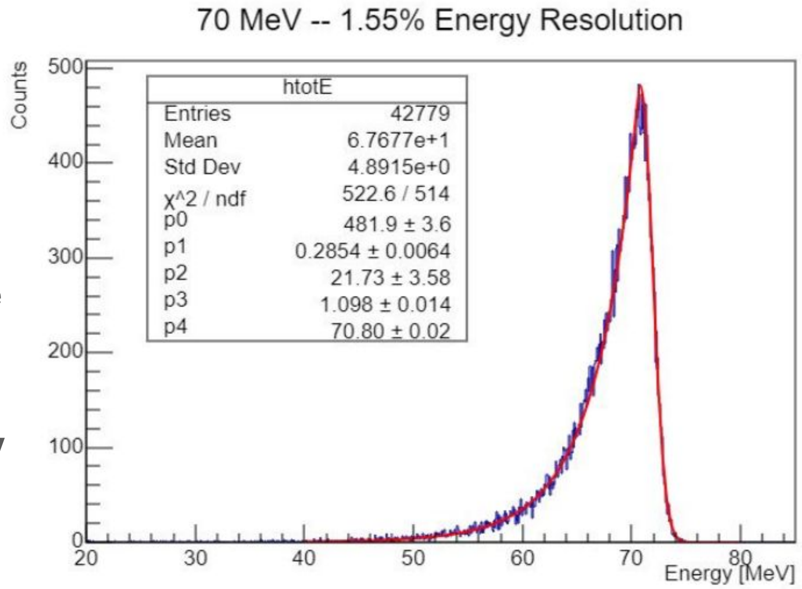

Citation: Omar Beesley, LYSO Updates/Answer
https://pioneer.npl.washington.edu/docdb/0003/000312/001/LYSO%20Updates_Answers%20%28General%20Meeting%2010_22_24%29.pdf

j.carlton@uky.edu

Timing Resolution Definition

- Use the strongest signal in an event as reference signal.
  - t_0 = time of peak
- In the same event find all crystal peaks t_i
  - Only use peaks above some energy threshold
- $\Delta t = t_0 - t_i$
  - The width of a gaussian fit to a histogram of all such measurements gives the timing resolution

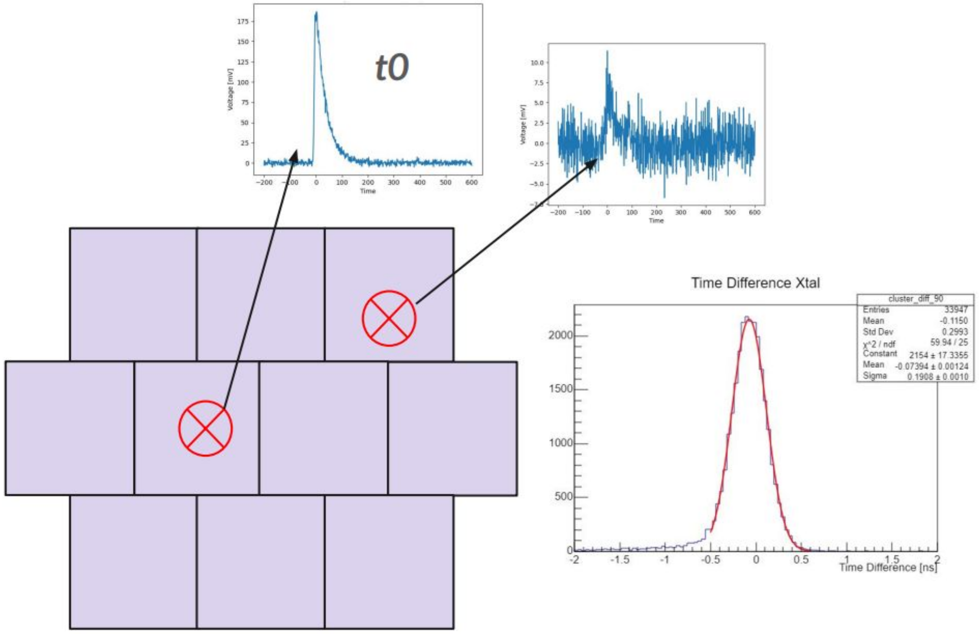

Citation: Measurements of a LYSO crystal array from threshold to 100 MeV, PIONEER collab (arxiv: 2409.14691)

j.carlton@uky.edu

Results - Energy Resolution

- Energy resolution is uniform near the center of the lyso array
- Towards the edges the energy resolution decreases due to leakage
  - In this case, into the NaI array

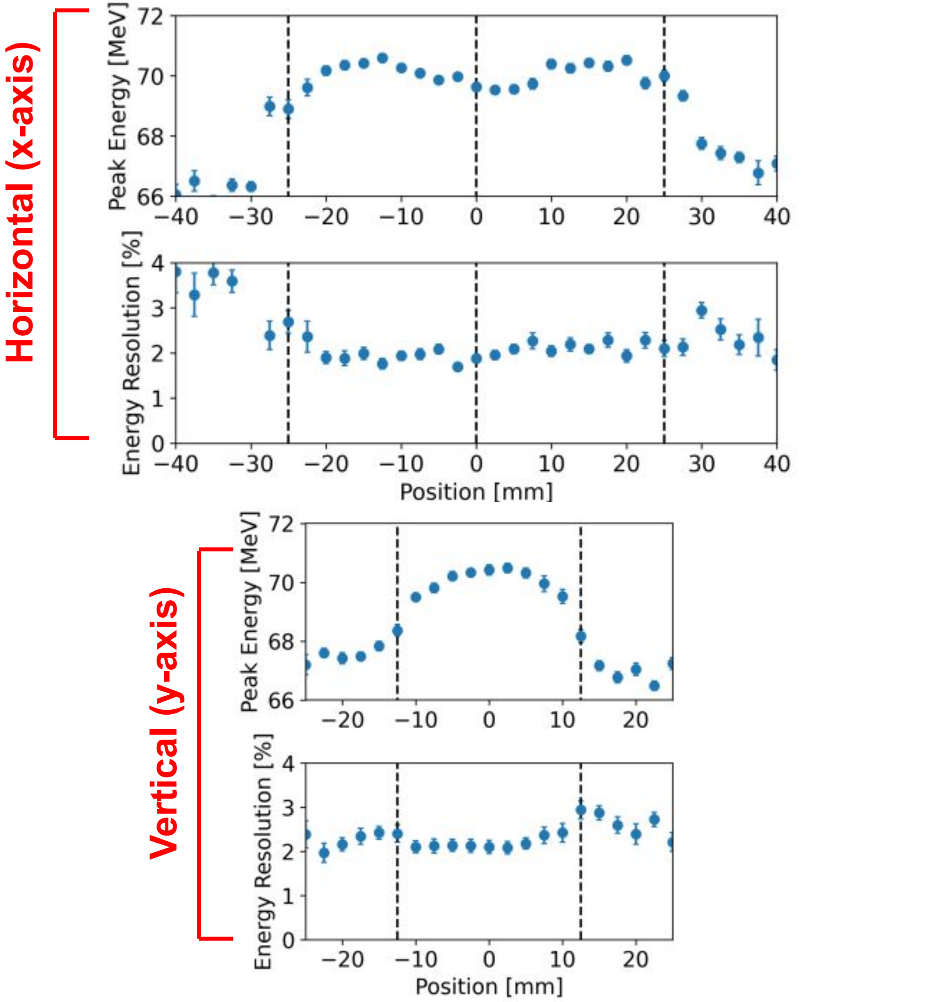

j.carlton@uky.edu

Results - Timing Resolution

- Timing resolution for 70 MeV events expected to be about 122.5 ps
- This measurement was largely influenced by noise from incorrect high voltage during test beam
  - Using a system of synchronized LEDs, clean, simultaneous signals were generated at UW
  - Improved timing resolution to about 60 ps
  - About that same as LXe

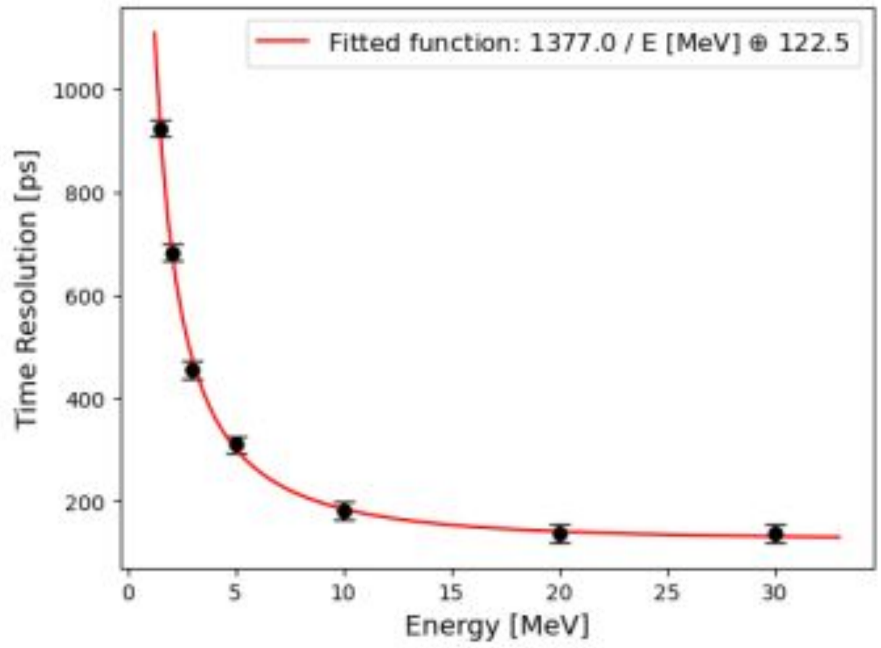

j.carlton@uky.edu

Compression and Entropy

 j.carlton@uky.edu

Data Set

- PSI Test beam, Run 1887
- 70 MeV/c centered on LYSO crystal 4.
- The data only includes lyso channels (no NaI for instance)
- More details on that run are in this elog (https://maxwell.npl.washington.edu/elog/pienuxe/R23/124)

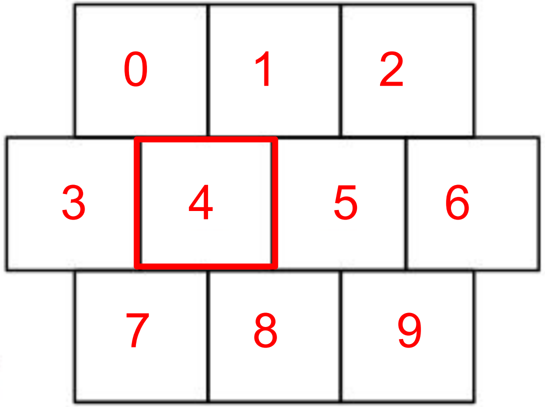

j.carlton@uky.edu

LYSO traces

- Select only LYSO channels and traces with a signal
- No pedestal subtraction, fitting, etc. (yet)

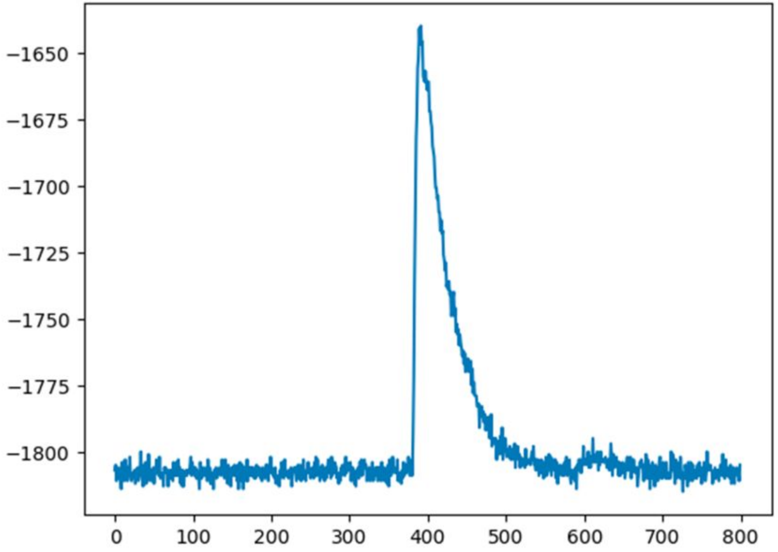

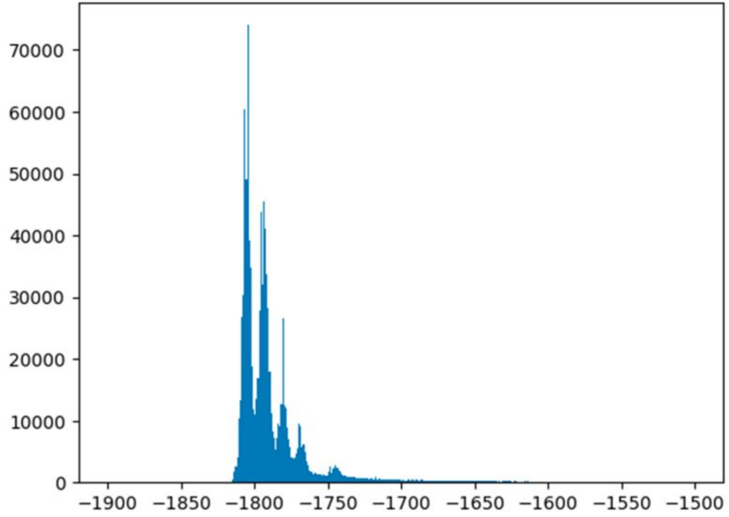

 j.carlton@uky.edu

Entropy and Lossless Compression

- For lossless compression, the best possible compression rate is the entropy rate
- To first order, the entropy of an entire trace is:

$$H(X_1, ..., X_n) = -\sum_{\text{traces}} p(X_1, ..., X_n) \log_2(p(X_1, ..., X_n))$$

- X_i is the random variable for the ADC value of the i^{th} sample in the trace with n samples
- If we assume X_i independent, then

$$H(X_1, ..., X_n) = H(X_1) + ... + H(X_n)$$

- By transforming ($X_i \rightarrow$ fit residuals), X_i becomes approximately independent

 j.carlton@uky.edu

Higher Order Entropy Estimations

- Assume we have N characters (traces) in our alphabet (data set)
- **Zero order:** each character in alphabet is statistically independent

$$H = \log_2(N)$$

- **First order:** each character in alphabet is statistically independent, p_i is the probability of that character to occur

$$H = -\sum_{i=1}^{N} p_i \log_2(p_i)$$

- **Second order:** $P_{j|i}$ is correlation between subsequent characters

$$H = -\sum_{i=1}^{N} p_i \sum_{j=1}^{N} P_{j|i} \log_2(P_{j|i})$$

- **General Model (impractical):** B_n represents the first n characters

$$H = \lim_{n \to \infty} \left[-\frac{1}{n} \sum p(B_n) \log_2(B_n) \right]$$

Citation: Joint Entropy, Wikipedia
https://en.wikipedia.org/wiki/Joint_entropy

j.carlton@uky.edu

Joint Entropy, Mutual Information

$$H(X_1, ..., X_n) \leq H(X_1) + ... + H(X_n)$$

Equality only holds if

$$X_1, ..., X_n \text{ are mutually statistically independent}$$

This means if

$$I(X_1, X_2) = H(X_1) + H(X_2) - H(X, Y) = 0$$

Then we must have X_1 and X_2 be statistically independent

j.carlton@uky.edu

Joint entropy for Independent Variables Proof

Statement:

$H(X_1, ..., X_n) = \sum_{i=1}^{n} H(X_i)$

Proof (part 1):

$$H(X_1, ..., X_n) = -\sum_{x_1,...,x_n} P(x_1, ..., x_n) \log_2(P(x_1, ..., x_n))$$

$$= -\sum_{x_1,...,x_n} P(x_1)...P(x_n) \left(\log_2(P(x_1)) + ... + \log_2(P(x_n))\right)$$

(Note: I am lazy, each $P(x_i)$ represents a different pdf in general)

j.carlton@uky.edu

Joint entropy for Independent Variables Proof

Proof (part 2):

$$H(X_1, ..., X_n) = -\left(\sum_{x_1} P(x_1)\log_2(P(x_1))\right)\left(\sum_{x_2} P(x_2)\cdot ...\cdot \sum_{x_n} P(x_n)\right)$$

$$- ...$$

$$-\left(\sum_{x_1} P(x_1)\cdot ...\cdot \sum_{x_{n-1}} P(x_{n-1})\right)\left(\sum_{x_n} P(x_n)\log_2(P(x_n))\right)$$

$$\text{Note } \sum_{x_i} P(x_i) = 1 \text{ and } \sum_{x_1} P(x_i)\log_2(P(x_i)) = H(X_i)$$

$$= H(X_1) + ... + H(X_n) \blacksquare$$

 j.carlton@uky.edu

Entropy estimation

- Average entropy per bit: 5.22 bits / sample (compare to 16 bits for a short)
- Samples near waveform edge have lower entropy
- Samples near middle have higher entropy, due to the pulses
- Entropy is nonzero b/c the waveforms are **not** identical: difference pedestals, different pulse sizes

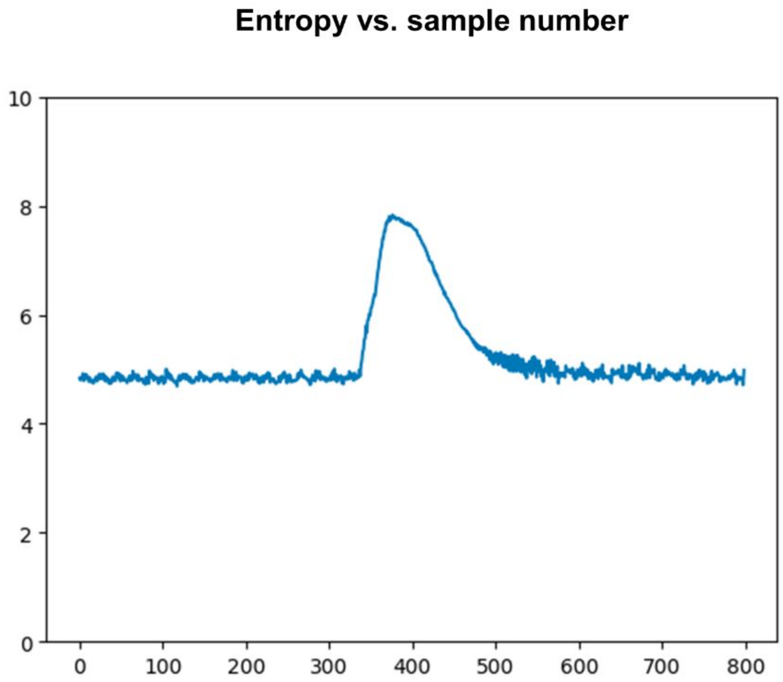

j.carlton@uky.edu

Pedestal subtracted

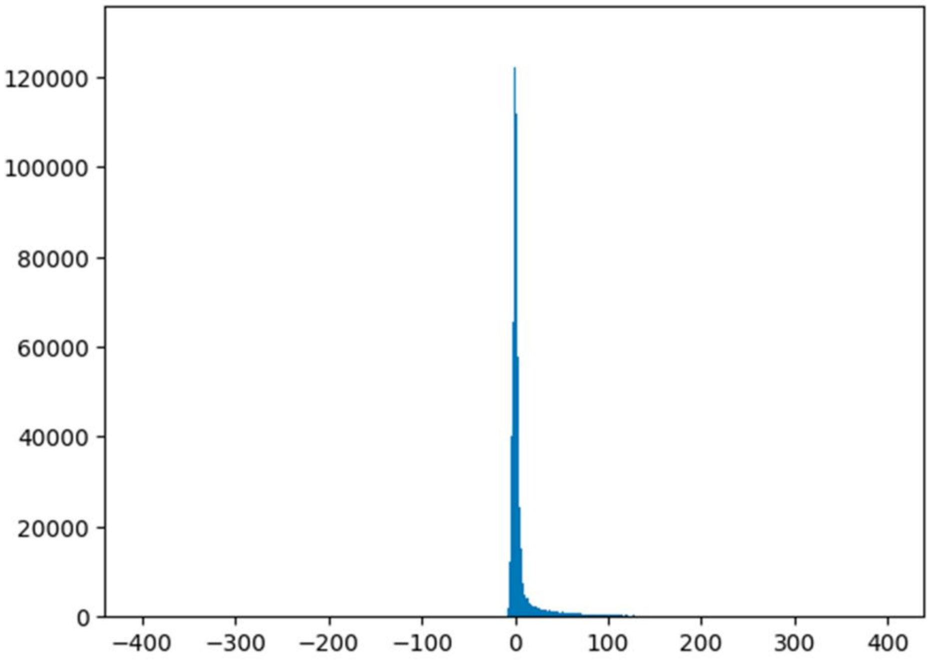

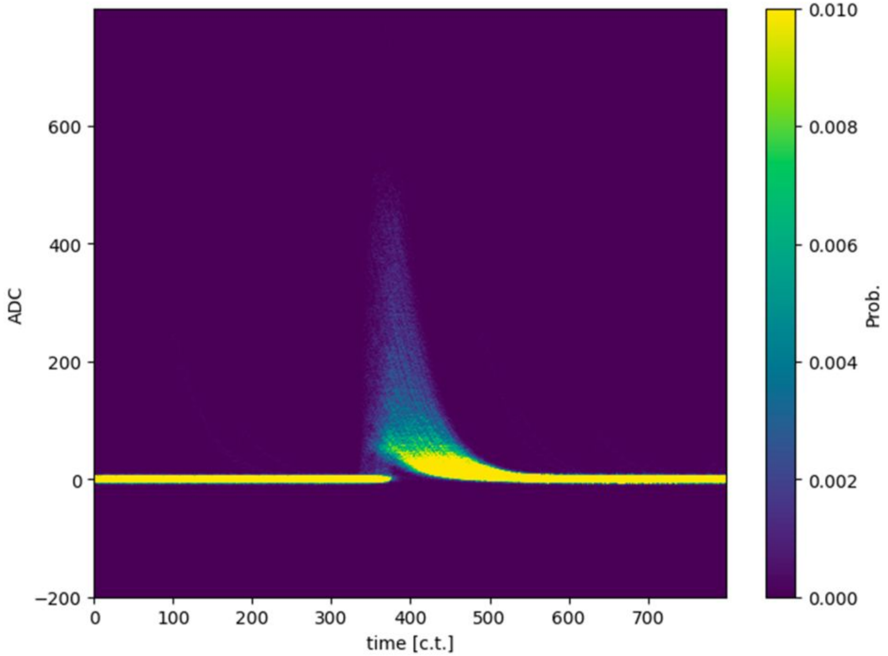

Entropy estimation

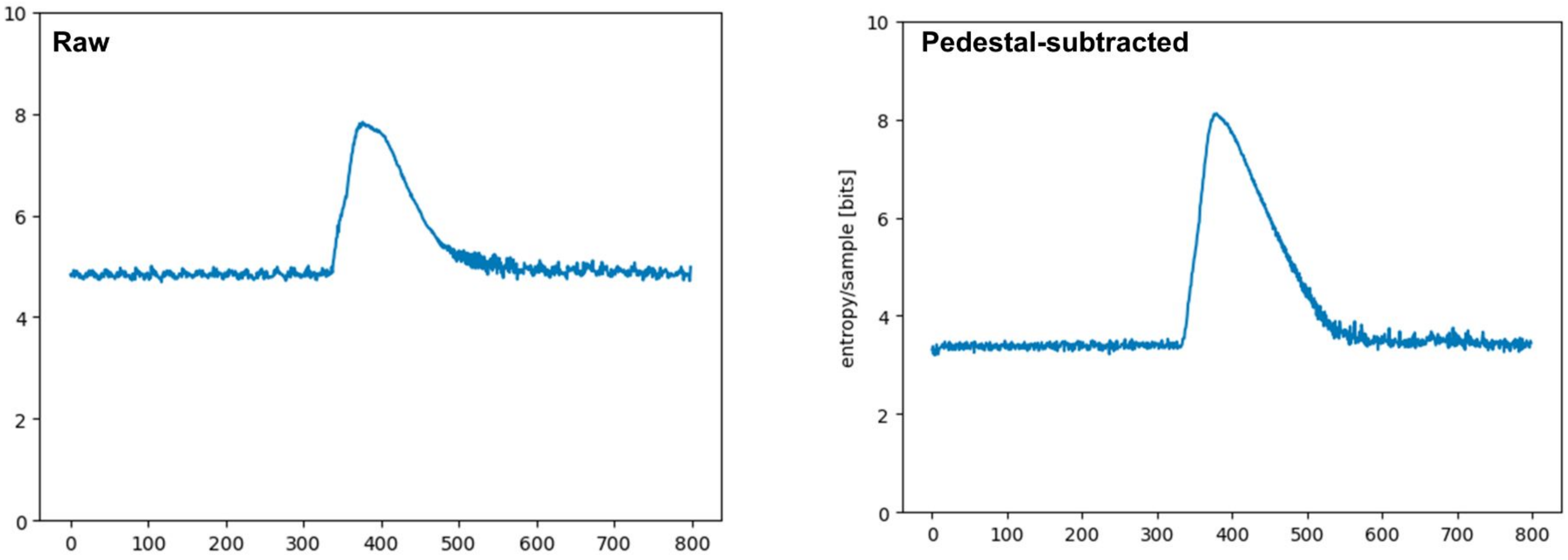

- Entropy reduced for samples near waveform edge: ~3.4 bits
- Average entropy per sample now: 4.05 bits/sample

 j.carlton@uky.edu

Discrete Gaussian entropy

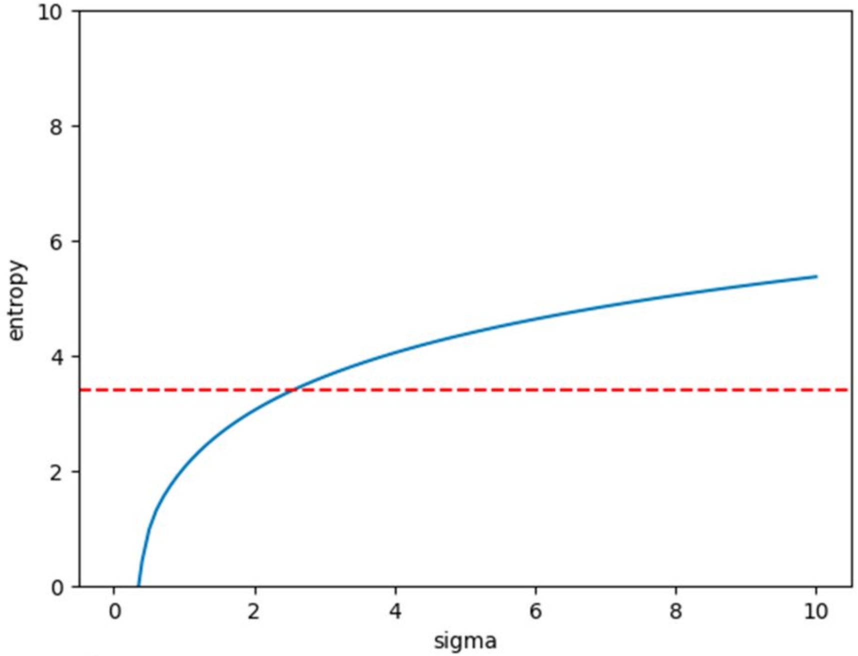

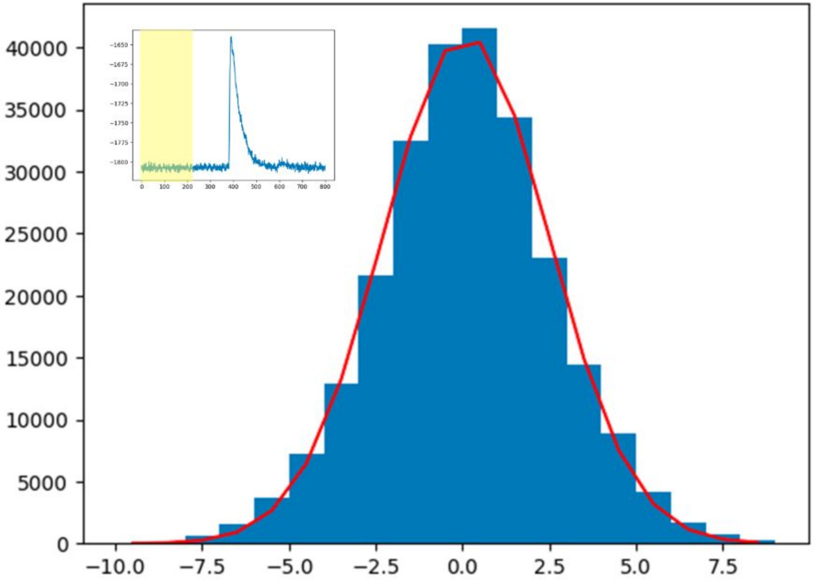

- If we assume gaussian noise: entropy of 3.4 bits -> $\sigma = 2.6$
- If we look at samples < samples number 200 and fit ADC to gaussian: $\sigma = 2.4$

j.carlton@uky.edu

Template fit

- Constructing a template
  - Normalized all traces
  - Time-align the peak
  - Smooth over adjacent sample
  - Fit with $f(t) = A \cdot T(t - t_0) + C$

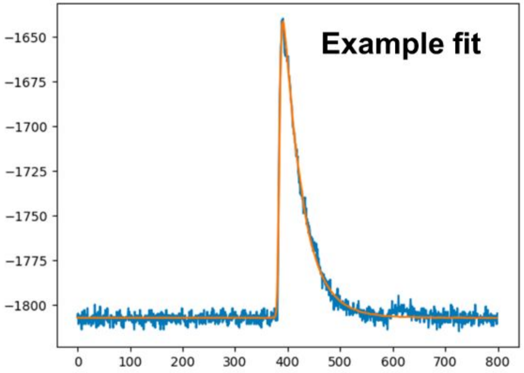

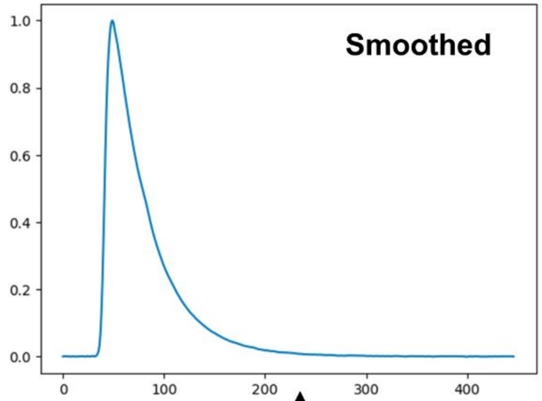

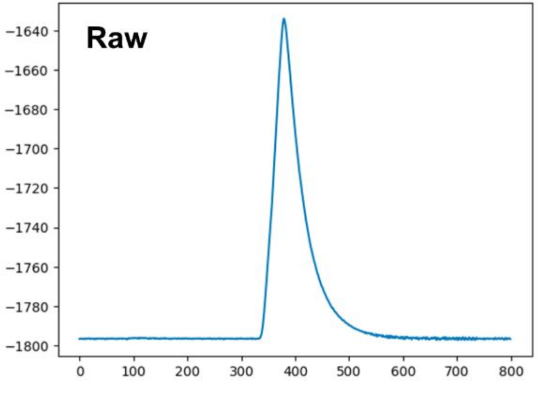

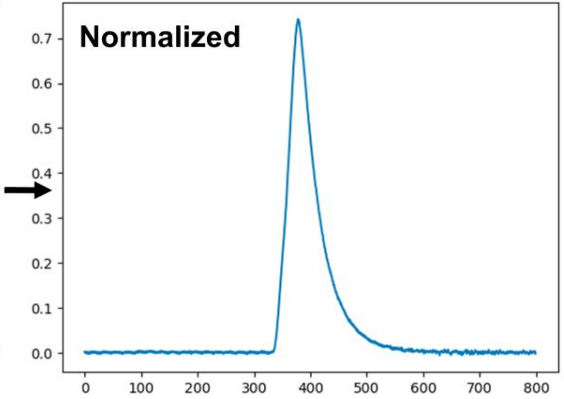

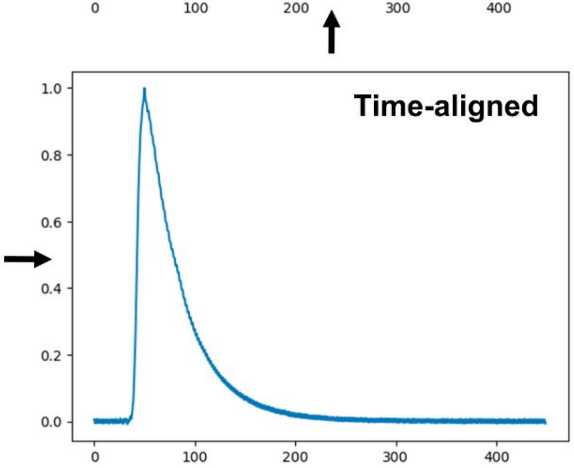

j.carlton@uky.edu

Template fit

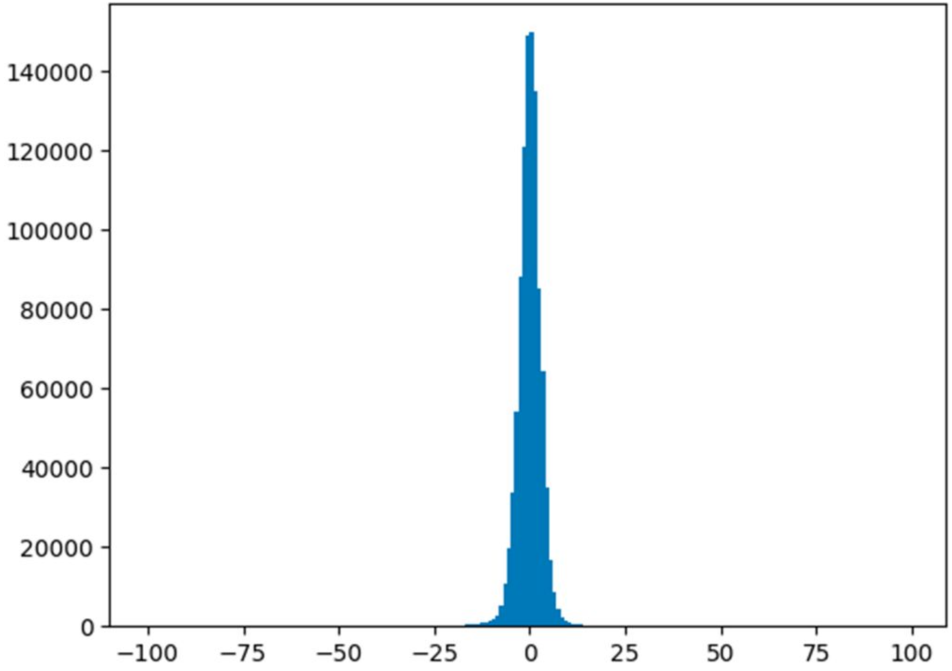

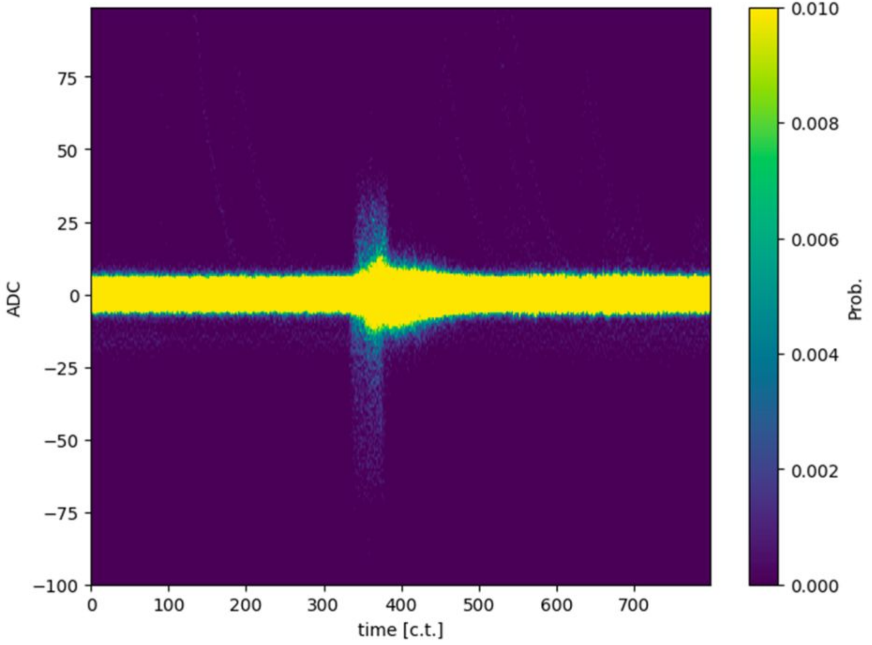

j.carlton@uky.edu

Entropy estimation

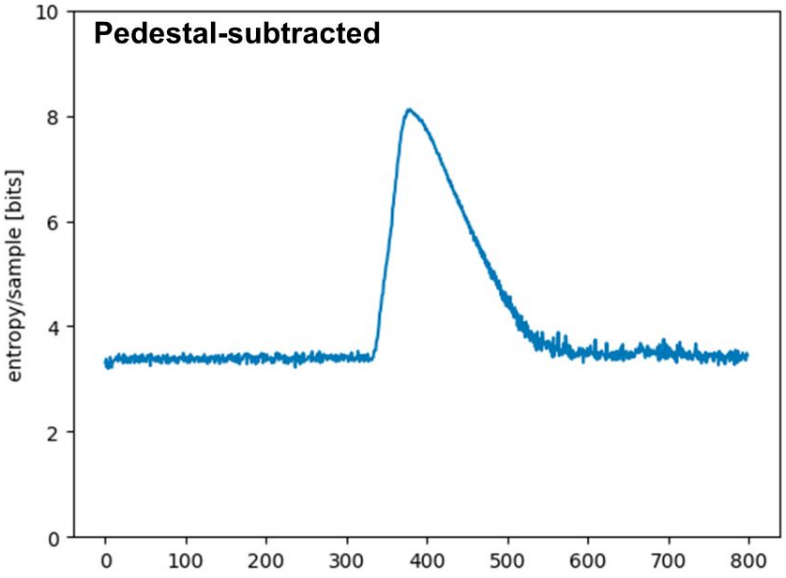

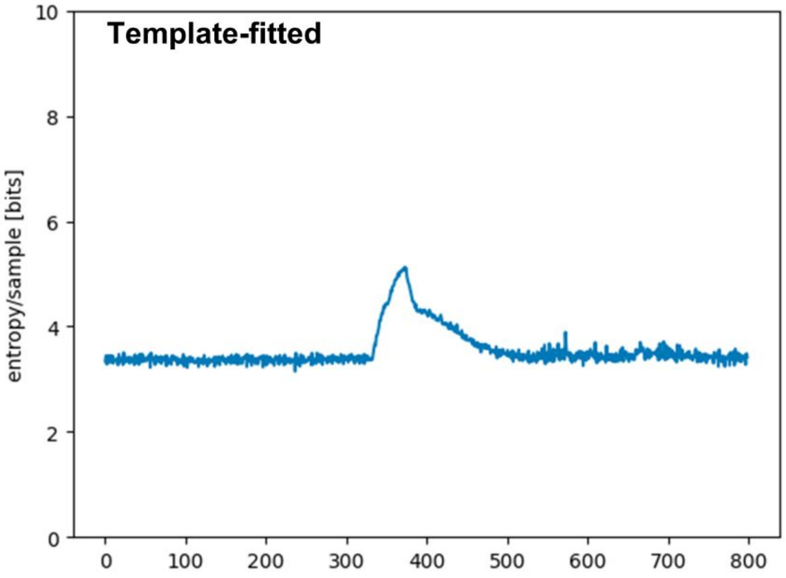

- Baseline hasn't changed much. Makes sense since fluctuations remain
- Peak in middle is reduced, but evidently we can still do better
- Average entropy per sample now: **3.55 bits/sample**

 j.carlton@uky.edu

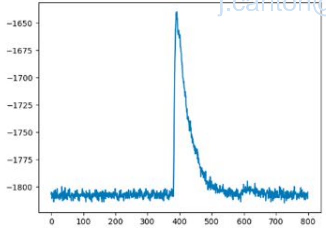

Correlations

Raw

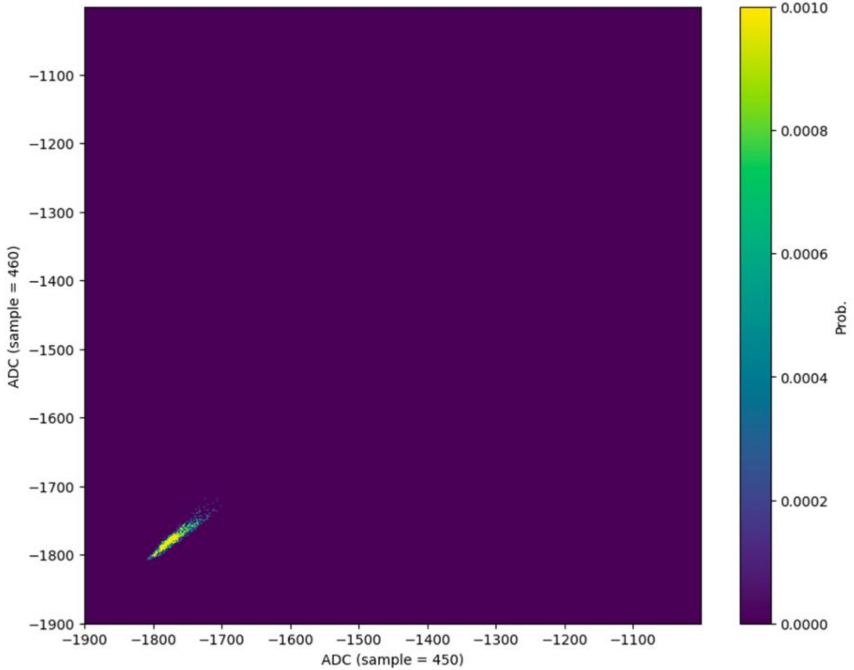

Templated-fitted

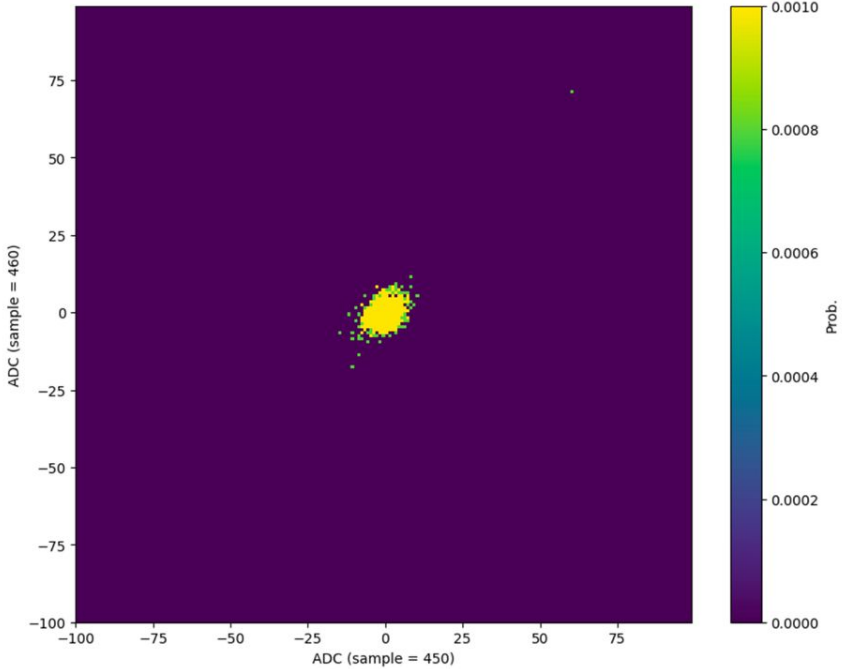

j.carlton@uky.edu

Mutual Information

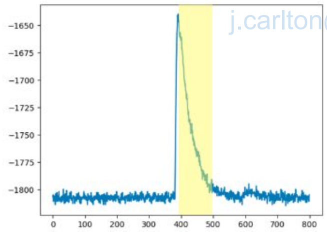

Raw

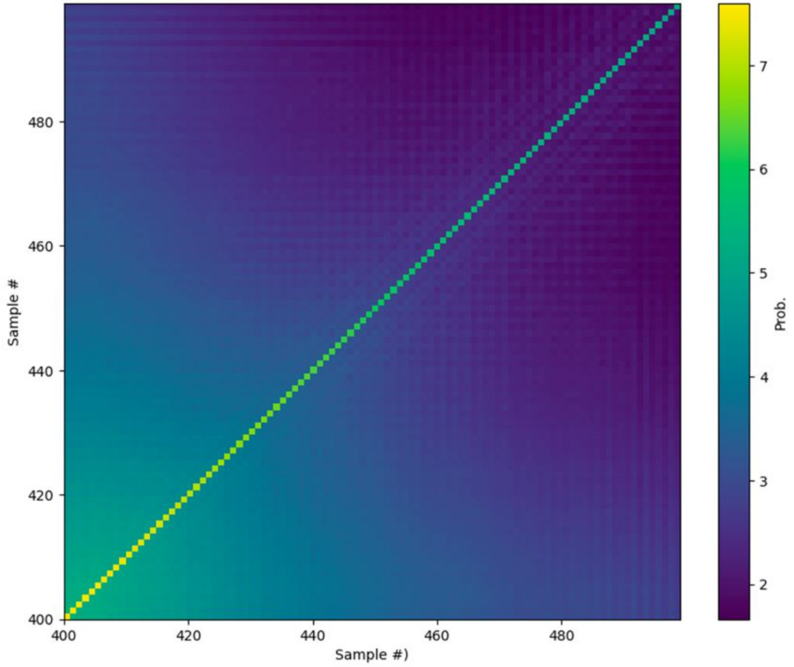

Templated-fitted

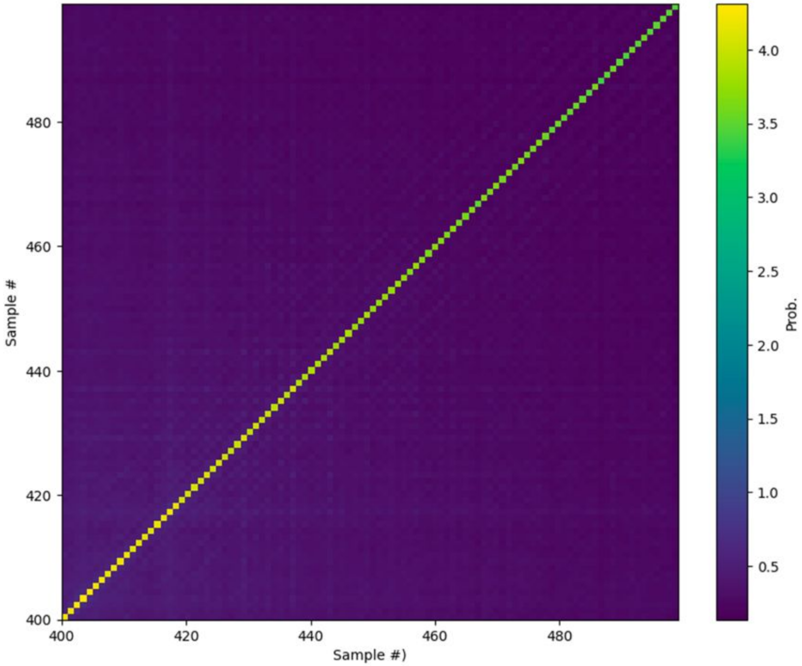

$H(X) + H(Y) - H(X,Y)$ **nonzero means there are still correlations**

 j.carlton@uky.edu

Template fitting going wrong

- What's causing the spread at the start of the pulse ~360 c.t. or so? (right plot)
- Seems like my template fit going wrong at the pulse turn-on

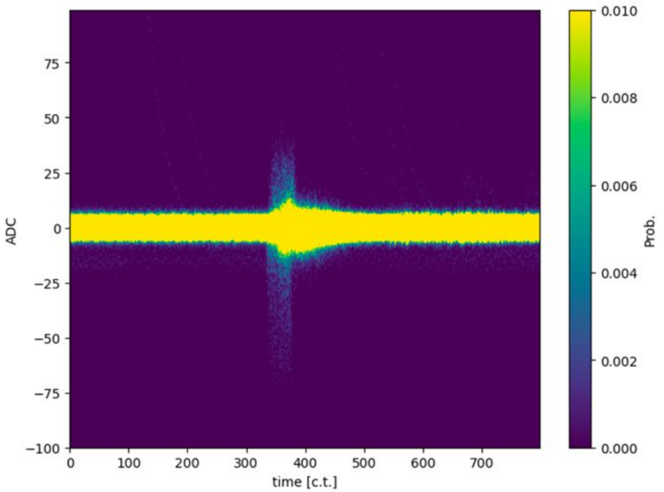

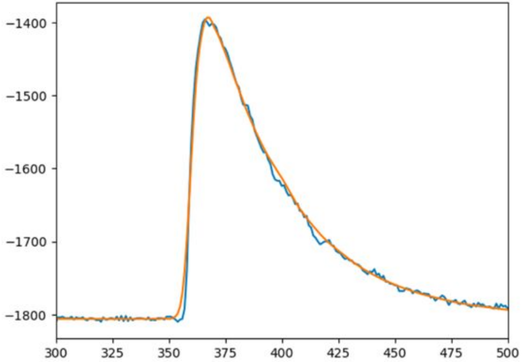

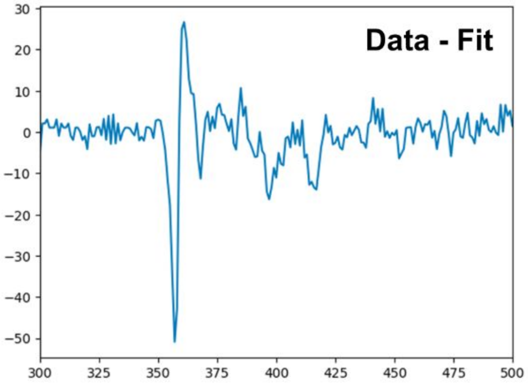

j.carlton@uky.edu

Stray point due to pileup

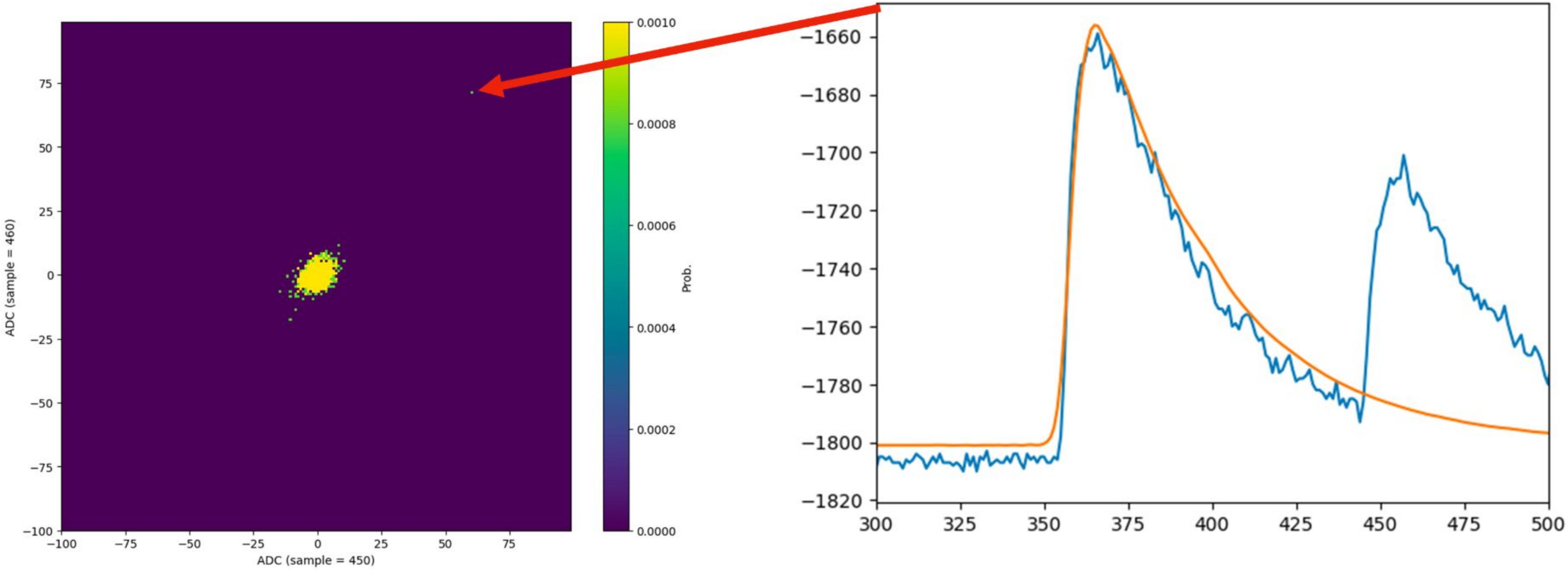

j.carlton@uky.edu

Mutual Information

- Mutual Information:
  $I(X_1, X_2) = H(X_1) + H(X_2) - H(X_1, X_2)$
- $I(X_1, X_2) = 0 \implies$ no correlation
- Template fitting reduces correlations between subsequent samples

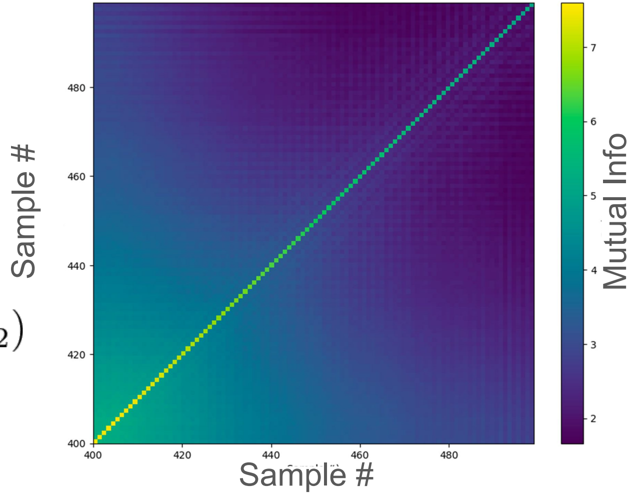

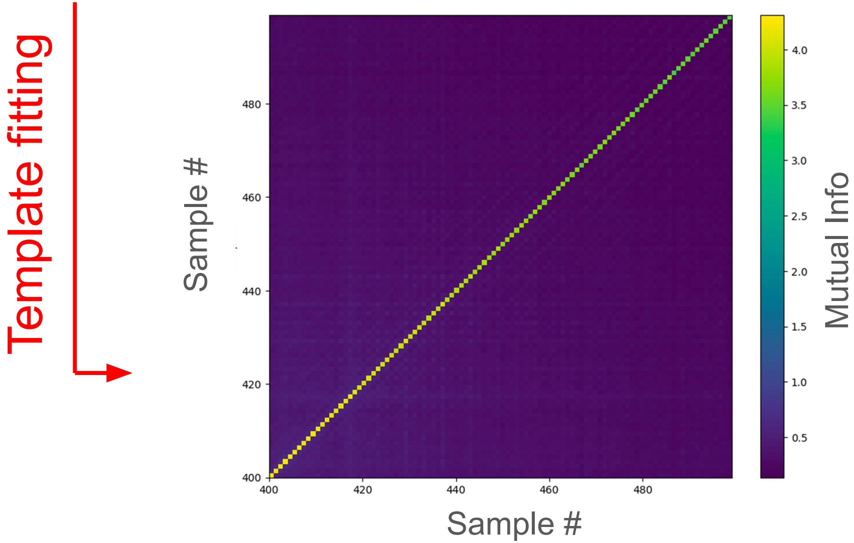

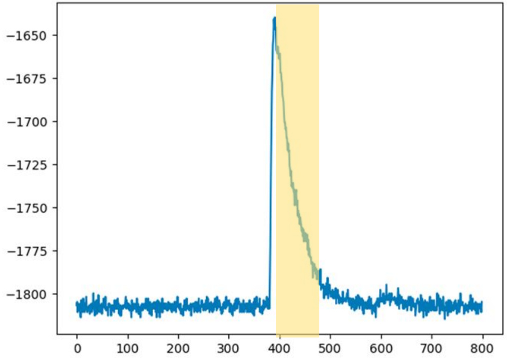

j.carlton@uky.edu

Entropy Estimation

- Average entropy:

$$H_{\text{avg}} = \frac{\sum_{i=1}^{N} H(X_i)}{N}$$

- In this case N = 800
- Before: H_{avg} = 5.22 bits/sample
- After: **H_{avg} = 3.55 bits/sample**
- Some room for improvement(?)

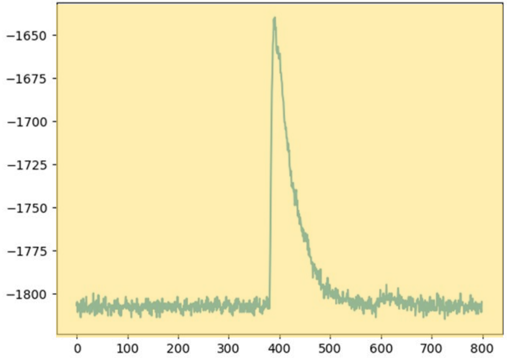

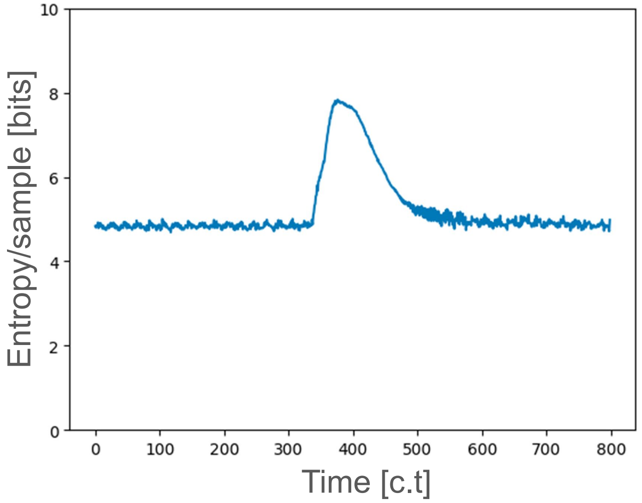

Template fitting

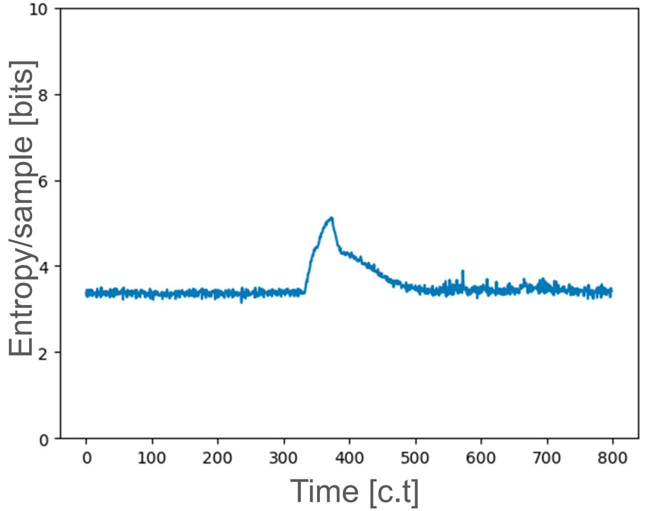

j.carlton@uky.edu

Explanation of Entropy Plot

- The pedestal is easy to fit, so the variance of the pedestal part of the signal is is just the noise of the WFD5s.
  - This is the minimum possible entropy when using this equipment
- The signal is harder to fit and therefore has more variance
  - Entropy of this part of the trace is therefore larger

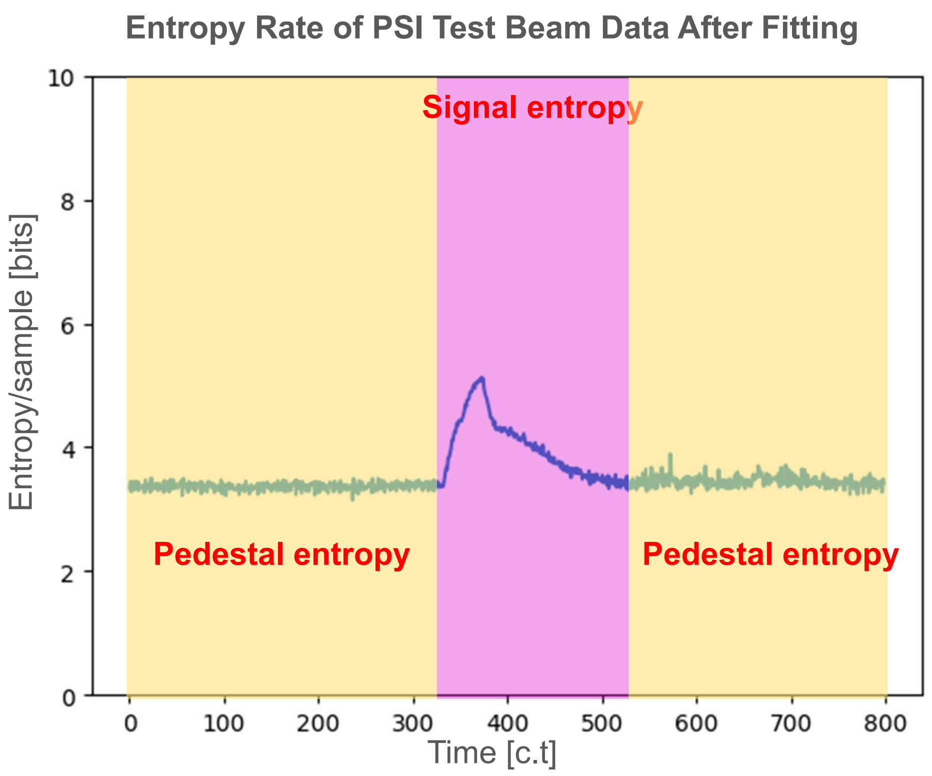

j.carlton@uky.edu

Theoretical Best Compression Calculation

Assuming data is sent as 12 bit ADC samples over PCIe at a data rate of 3.5 GB/s:

$$\text{Compression Ratio} = \frac{\text{Entropy Rate}}{12}$$

$$\text{Storage Data Rate} = \text{Compression Ratio} \cdot 3.5\ \text{GB/s}$$

Entropy rate = 3.4 → New Data Rate ≈ 0.99 GB/s

Entropy rate = 5 → New Data Rate ≈ 1.46 GB/s

j.carlton@uky.edu

Continuing Support for Test Stand DAQ

- Institutions that currently use or plan to use the test stand DAQ in some capacity:
    - CENPA at University of Washington
    - TRIUMF, Canada
    - PSI, Switzerland

- Maintaining and developing software to fit specific needs of each institution

j.carlton@uky.edu

Signal Conditioning

- Want a narrow distribution for compression. Let r_i be the numbers we compress
- Methods tried:
  - No conditioning
  - Delta encoding: $r_i = y_{i+1} - y_i$
  - Twice Delta Encoding: $r_i = y_{i+2} - 2y_{i+1} + y_i$
  - Double Exponential Fit: $r_i = y_i - (A \cdot \exp(at_i) + B \cdot \exp(bt_i))$
  - **Shape Fit**: $\mathbf{r_i = y_i - (A \cdot T(t_i - t_0) + B)}$

No Conditioning

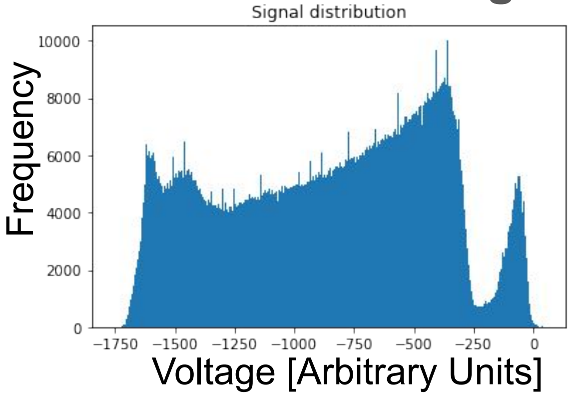

Shape Fit

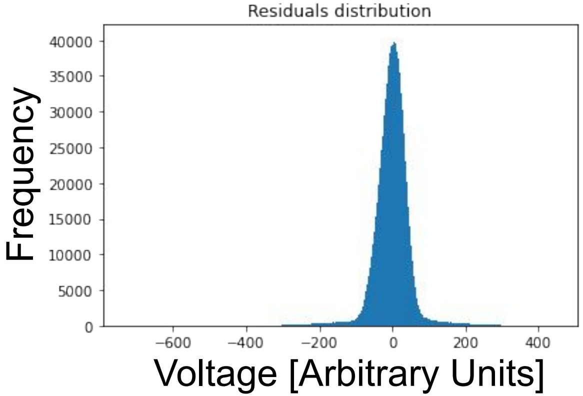

j.carlton@uky.edu

Shape Fitting Algorithm

1. Construct a discrete template from sample pulses
2. Interpolate template to form a continuous Template, *T(t)*
3. "Stretch" and "shift" template to match signal:

$$X[i] = a(t_0)T(t[i] - t_0) + b(t_0)$$

   [Note: a and b can be calculated explicitly given t_0]

4. Compute χ^2 (assuming equal uncertainty on each channel i)

$$\chi^2 \propto \sum_i \{X[i] - a(t_0)T(t[i] - t_0) + b(t_0)\}^2$$

5. Use Euler's method to minimize χ^2

j.carlton@uky.edu

Lossless Compression Algorithm

- Rice-Golomb Encoding
  - Let x be number to encode
    y = "s"+"q"+"r"
    - q = x/M (unary)
    - r = x%M (binary)
    - s = sign(x)
  - Any distribution
  - Close to optimal for valid choice of M
  - One extra bit to encode negative sign
  - Self-delimiting
  - If quotient too large, we "give up" and write x in binary with a "give up" signal in front

Rice-Golomb Encoding (M=2)

Value	Encoding
-1	011
0	000
1	001
2	1000

Red = sign bit
Blue = quotient bit(s) (Unary)
Yellow = remainder bit (binary)

j.carlton@uky.edu

How to choose Rice-Golomb parameter M

- Generated fake Gaussian data (centered at zero) with variance σ^2
- For random variable X, $M \approx \text{median}(|X|)/2$ is a good choice
  - This is the close to the diagonal on the plot
- $\sigma \approx 32$ for residuals of shape on wavedream data → M = 16 is a good choice

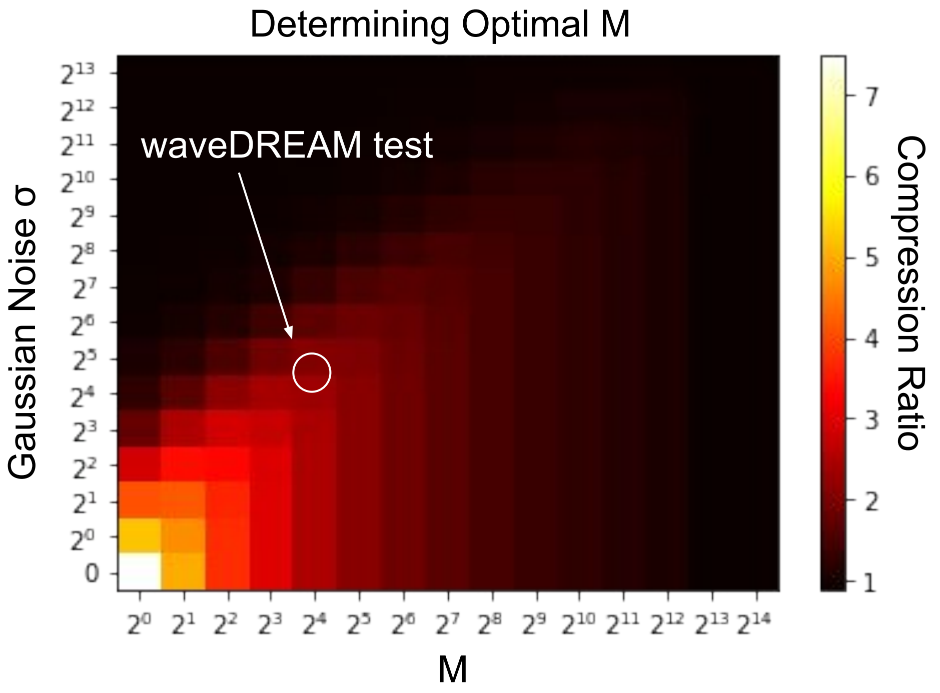

j.carlton@uky.edu

Compression Ratio from Rice-Golomb Encoding

- Lossless compression factor of ~2
- In agreement with plot from simulated data on last slide
- Best compression ratio we achieved

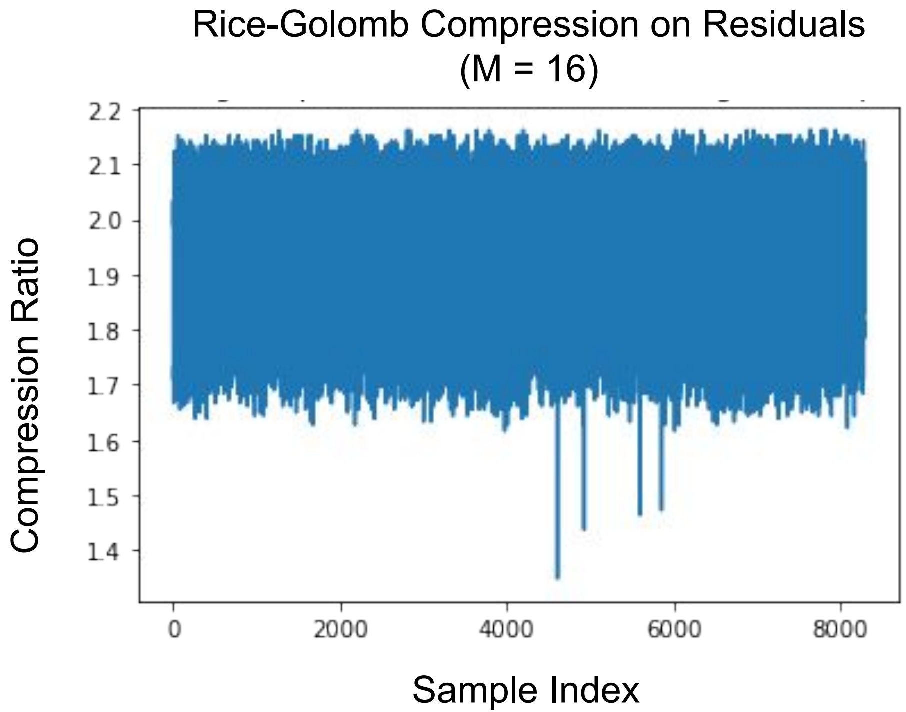

j.carlton@uky.edu

Real Time Compression Algorithm

- We choose to let the FE's GPU and CPU handle compression for flexibility

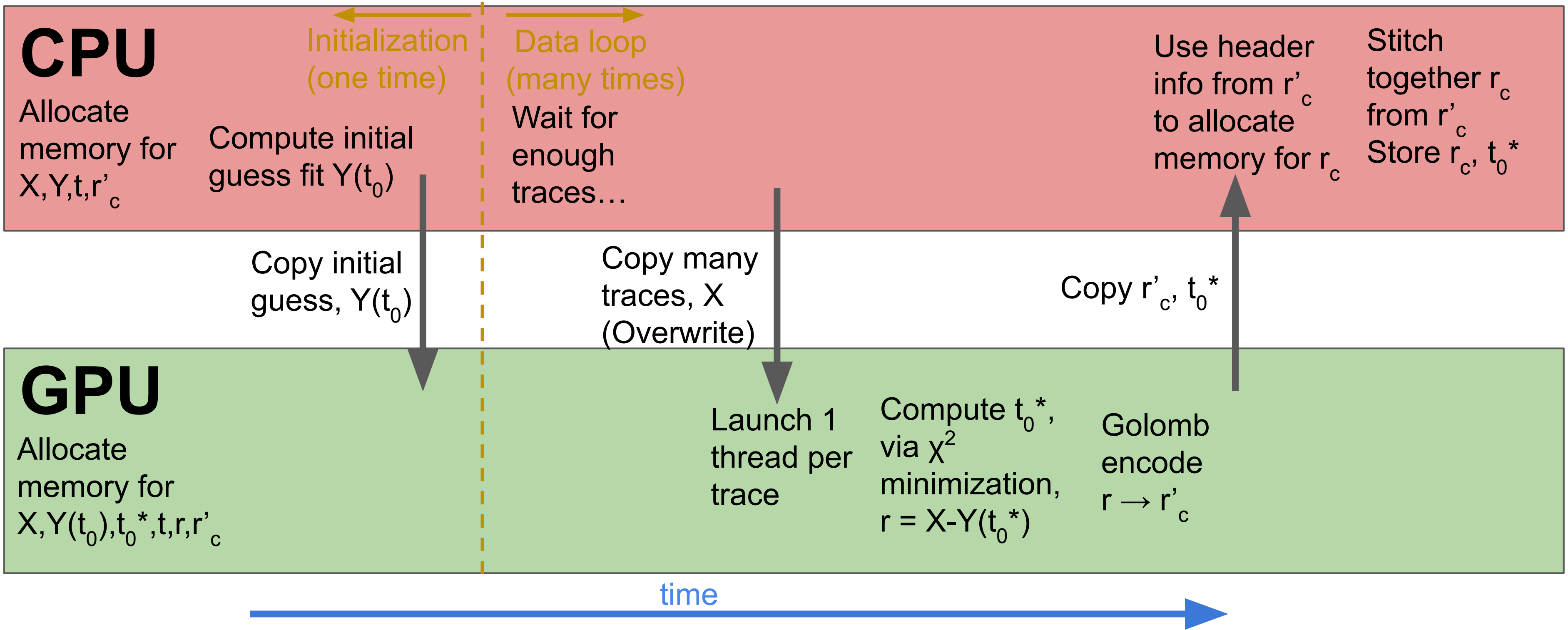

j.carlton@uky.edu

GPU Benchmarking (Timings)

- Block Size:
  - A GPU parameter, number of threads per multiprocessor

- Can compress 2^{26} integers (32-bit) in roughly ⅓ of a second. → ~ **0.8 GB/s** compression rate

Fit + Compression Time using A5000 in PCIe4 (Batch Size = 1024)

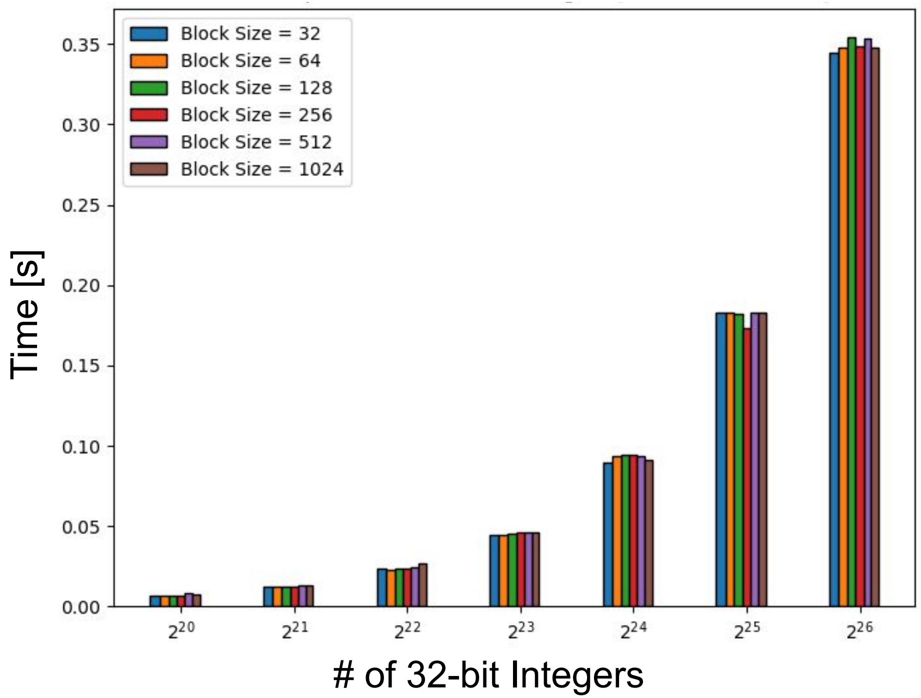

j.carlton@uky.edu

GPU Benchmarking (Timings)

- Batch Size:
  - How many integers are compressed by a single GPU thread
- Data must be sent to GPU in batches (not a continuous flow) to take full advantage of parallel computation